CHIRAL SYMMETRY BREAKING IN MOLECULES AND SOLIDS

T. Nattermann
University of Cologne

* F.Li, TN and V. Pokrovsky Phys. Rev.Lett. **108**, 107302 (2012)
TN arXiv:1210.1358

Acknowledgments to SFB 608 of DFG.

Outline

Introduction

Hund's Paradox

A second paradox

Symmetry breaking in chiral magnets

Topological defects in chiral magnets

Conclusions

Chirality

handedness: object and mirror image do not agree

enantiomers,
optical isomers

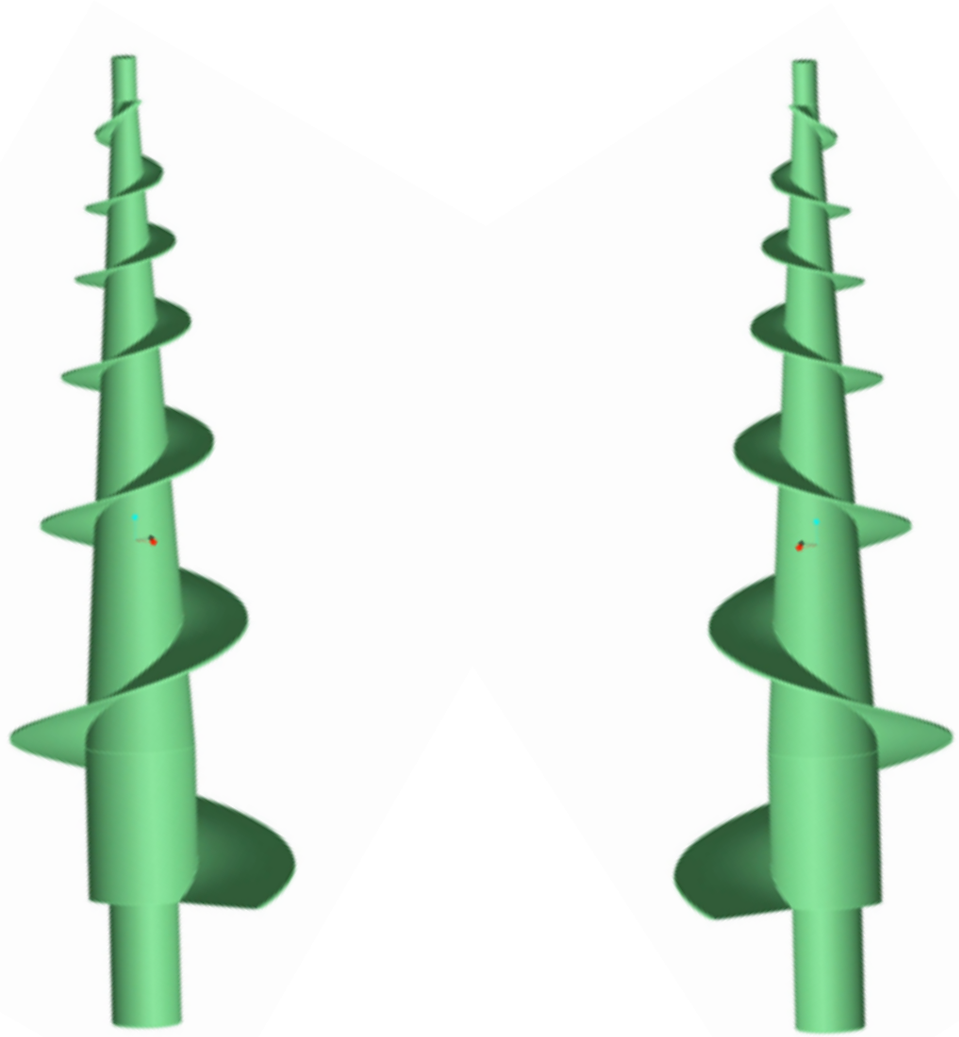

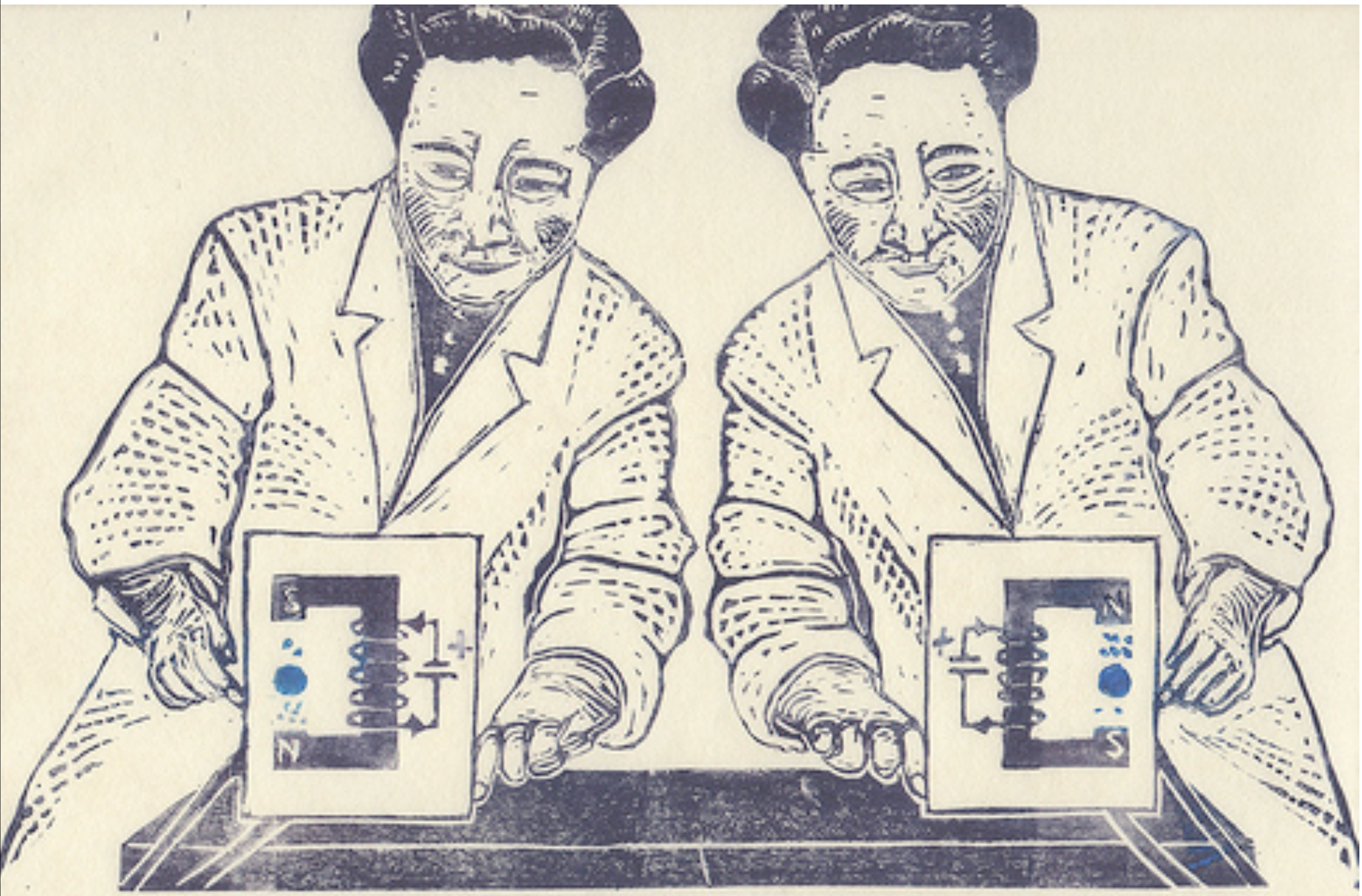

2/10

Madame Wu and the Violation of Parity

Ellie Williams-Ruby
2011

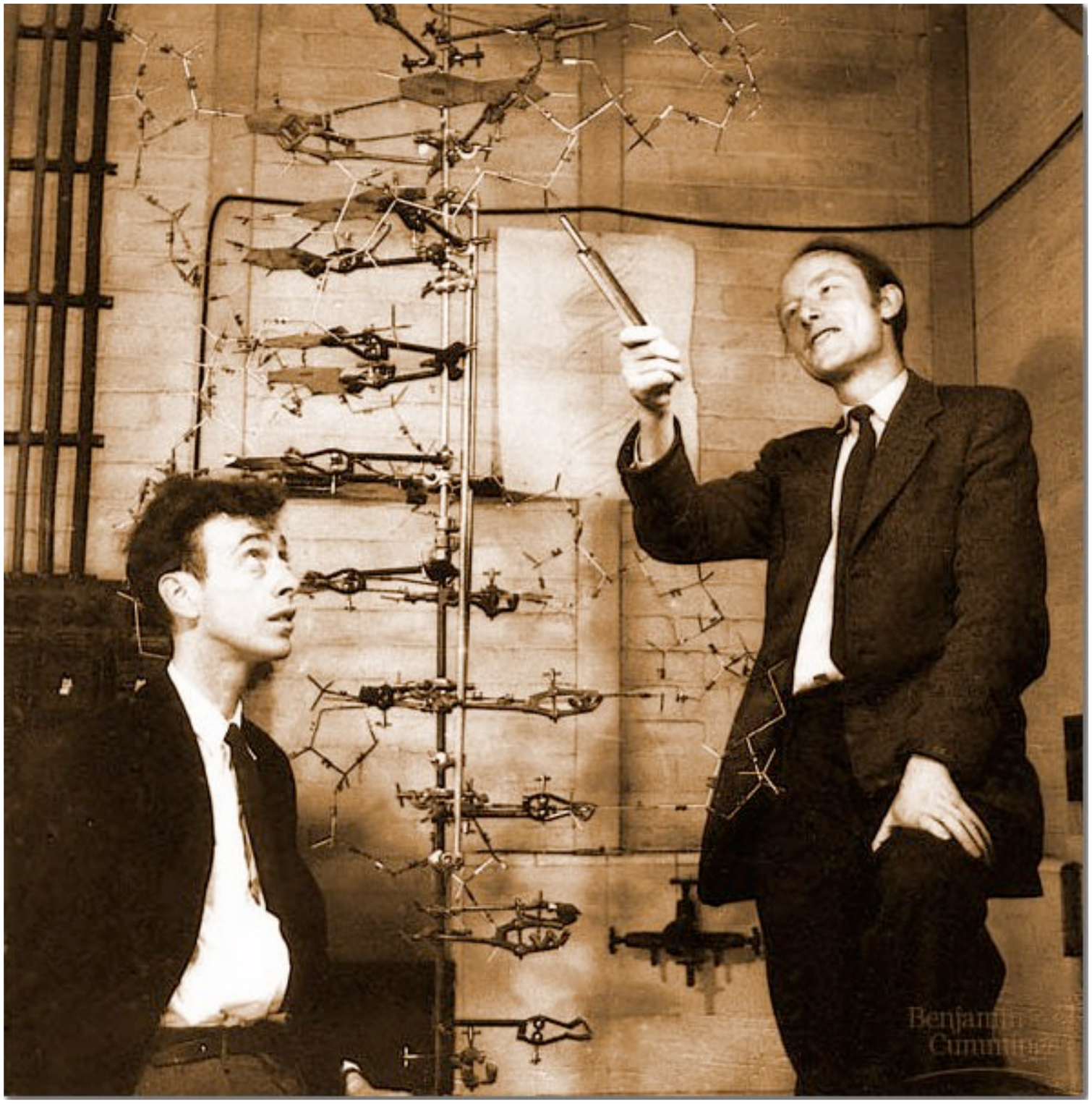

MOLECULAR STRUCTURE OF NUCLEIC ACIDS

A Structure for Deoxyribose Nucleic Acid

WE wish to suggest a structure for the salt of deoxyribose nucleic acid (D.N.A.). This structure has novel features which are of considerable biological interest.

J. D. WATSON
F. H. C. CRICK

Medical Research Council Unit for the Study of the Molecular Structure of Biological Systems, Cavendish Laboratory, Cambridge.

April 2.

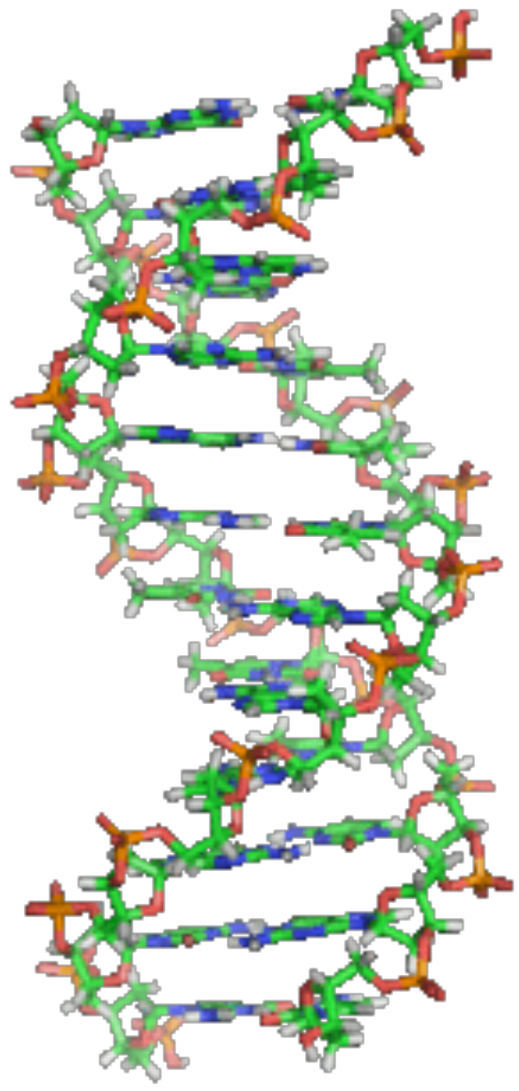

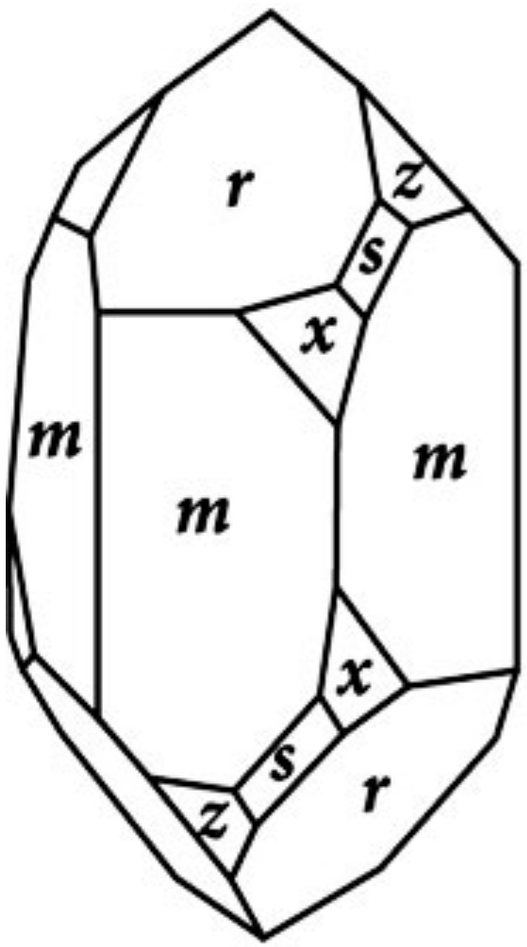

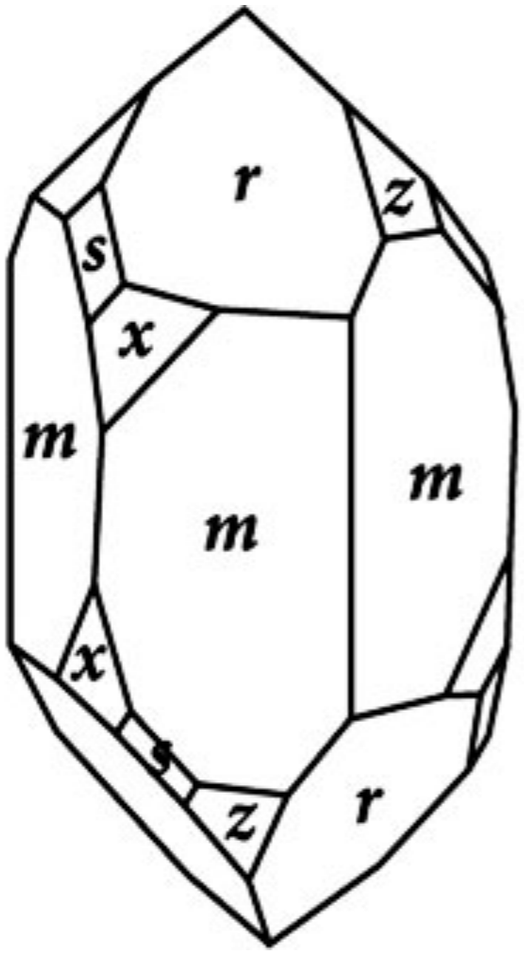

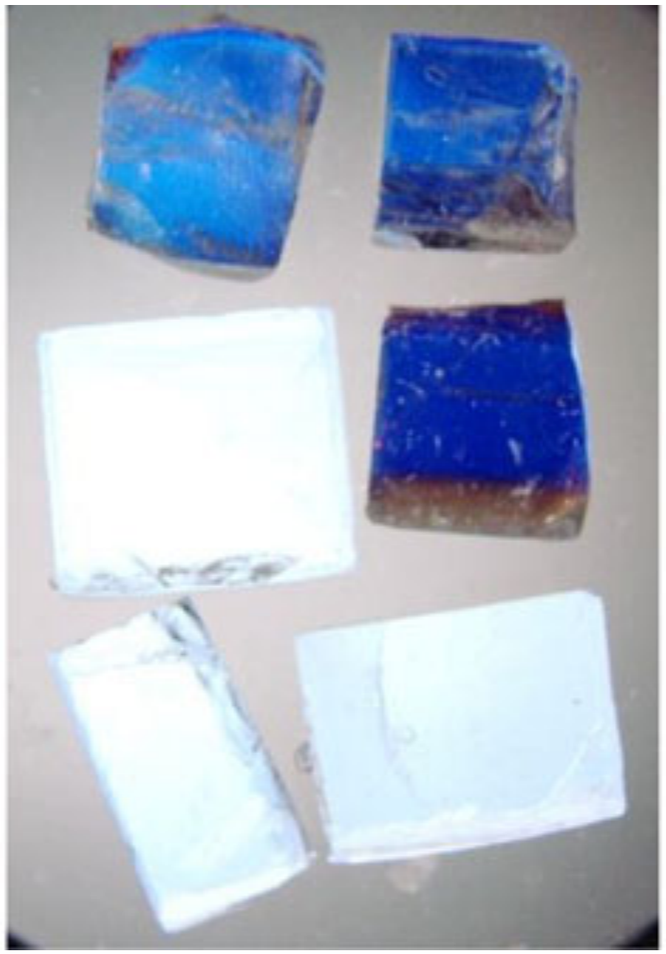

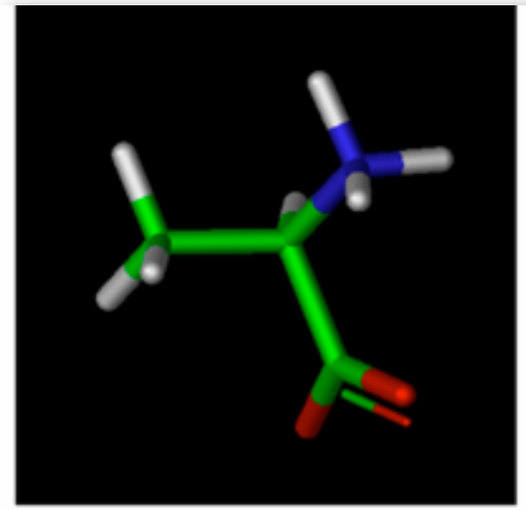

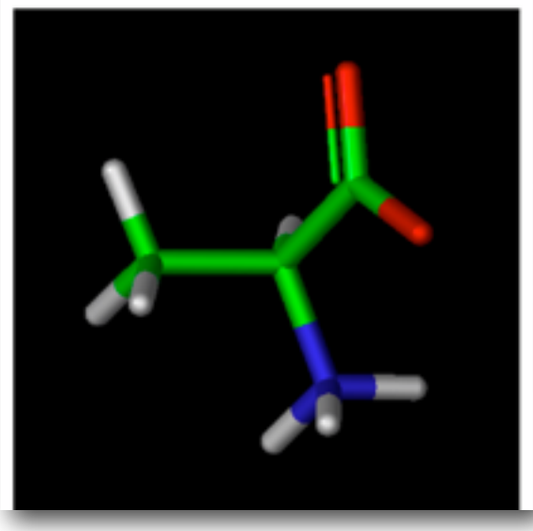

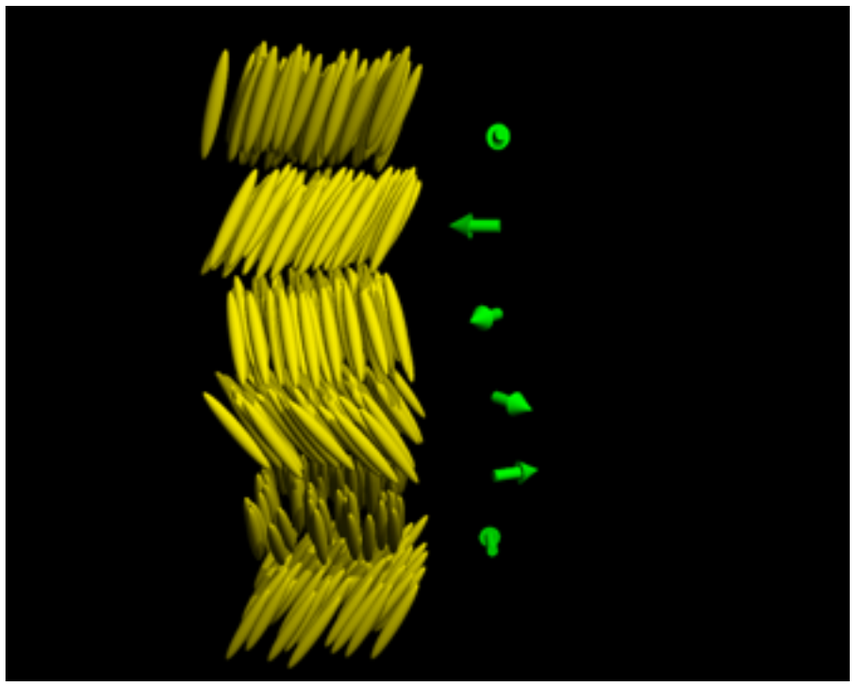

Examples of chiral substances. (a) Schematic of d and l quartz. (b) Sodium chlorate crystal, and (c) D (upper) and L (lower) alanine. In (b), d and l crystals are differentiated by their color under polarized light.

August 1972, Volume 177, Number 4047

SCIENCE

More Is Different

Broken symmetry and the nature of the hierarchical structure of science.

P. W. Anderson

The chemists will tell you that ammonia "is" a triangular pyramid

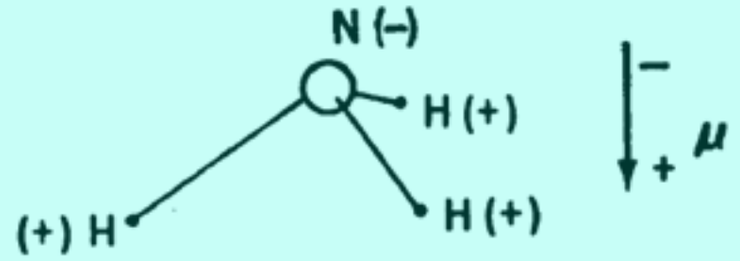

with the nitrogen negatively charged and the hydrogens positively charged, so that it has an electric dipole moment (μ), negative toward the apex of the pyramid. Now this seemed very strange to me, because I was just being taught that nothing has an electric dipole moment. The professor was really proving that no nucleus has a dipole moment, because he was teaching nuclear physics, but as his arguments were based on the symmetry of space and time they should have been correct in general.

Hund's Paradox: molecules and solids built by Coulomb interaction

Parity transformation:

$$\hat{P}\mathbf{r} = -\mathbf{r}$$

$$\hat{P}\mathbf{E} = -\mathbf{E}$$

$$\hat{P}\mathbf{B} = \mathbf{B}$$

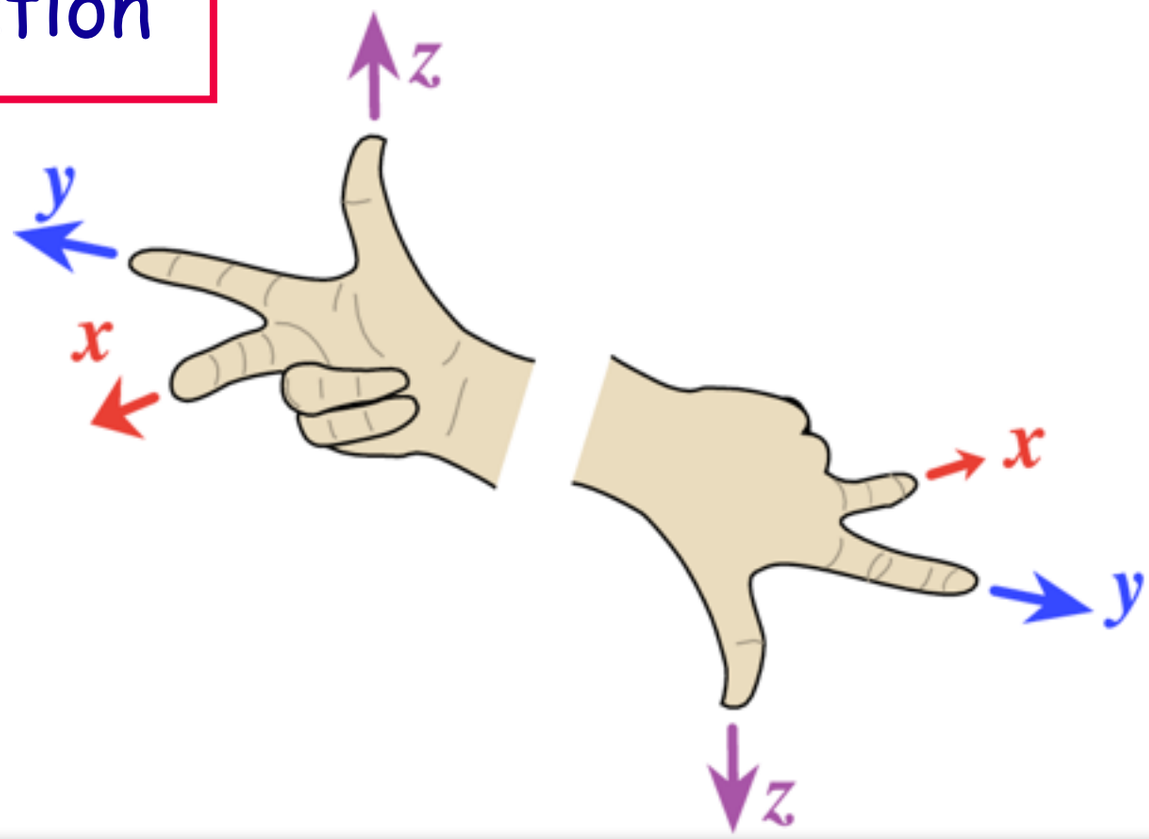

$$\boldsymbol{\nabla} E = \rho$$

$$\boldsymbol{\nabla} B = 0$$

$$\boldsymbol{\nabla} \times \mathbf{E} = \frac{1}{c}\dot{\boldsymbol{B}}$$

$$\boldsymbol{\nabla} \times \mathbf{B} = \frac{1}{c}\boldsymbol{j} + \frac{1}{c}\dot{\boldsymbol{E}}$$

$$m\ddot{\mathbf{r}} = e\boldsymbol{E} + \frac{e}{c}\dot{\boldsymbol{r}} \times \boldsymbol{B}$$

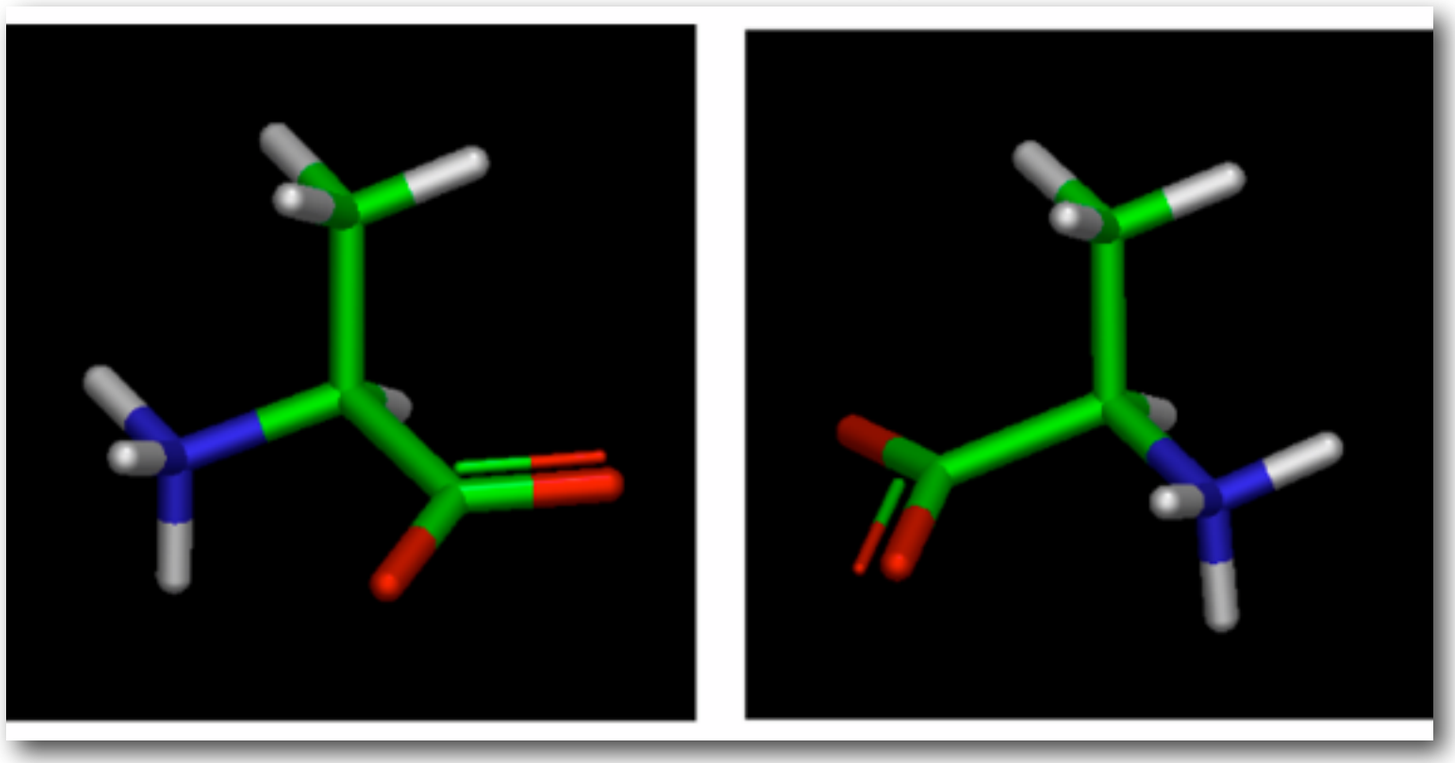

Zur Deutung der Molekelspektren. III.

Bemerkungen über das Schwingungs- und Rotationsspektrum bei Molekeln mit mehr als zwei Kernen.

Von **F. Hund** in Göttingen.

Mit 7 Abbildungen. (Eingegangen am 28. Mai 1927.)

Im Falle, daß eine vier- oder mehratomige Molekel zwei spiegelbildlich gleiche Anordnungen tiefster potentieller Energie hat, sind diese in jedem stationären Zustand in gleicher Weise vorhanden. Dem Übergang aus der einen Anordnung in das Spiegelbild entspricht eine Frequenz. Diese Tatsache steht mit der Existenz der optischen Isomere nicht im Widerspruch. Die bei gleichen Kernen auftretende Einteilung in nichtkombinierende Termsysteme ergibt sich für die Schwingung durch Betrachtung der Normalkoordinaten; für die Rotation folgt sie aus den Eigenschaften der Eigenfunktionen des Kreisels.

Wir können also sagen: Wenn bei einer Molekel zwei einander spiegelbildlich entsprechende und verschiedene Anordnungen der Kerne möglich sind, so sind die stationären Zustände nicht Bewegungen in der Nähe einer der beiden Gleichgewichtsanordnungen. Jeder stationäre Zustand ist vielmehr aus Rechts- und Linksanordnungen gleichmäßig zusammengesetzt. Bei den höher angeregten Schwingungen ist die mitt-

Leipzig 1929-1946

Hund's explanation

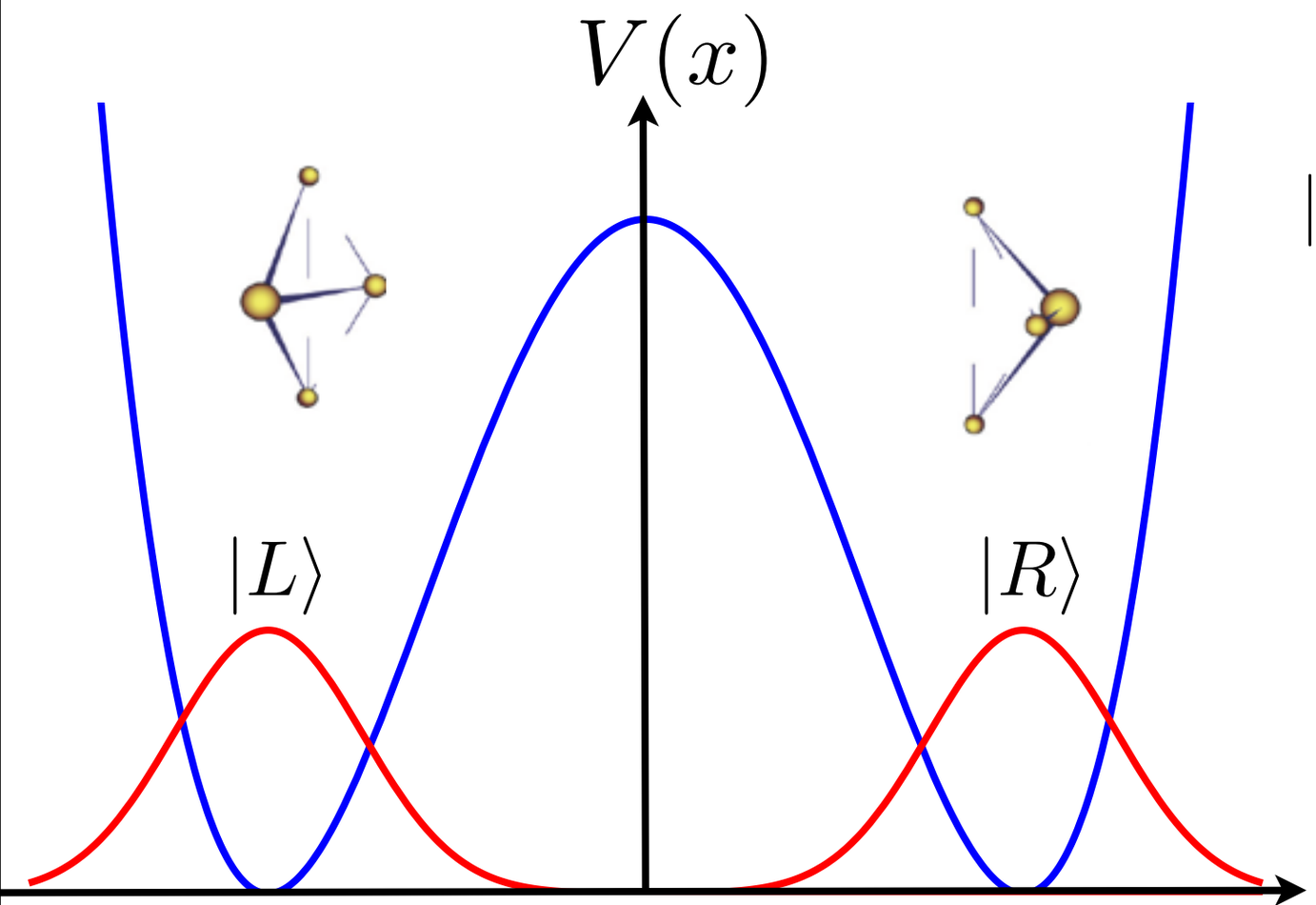

$|R\rangle, |L\rangle$ harmonic oscillator states

$$\hat{\mathcal{H}} = \omega \mathbf{1} + \Omega \boldsymbol{\sigma}_x$$

$$|\pm\rangle = \tfrac{1}{\sqrt{2}}(|R\rangle \pm |L\rangle)$$

$$\epsilon_\pm = \omega \mp \Omega, \quad \omega \gg \Omega$$

prepare system at $t = 0$ in $|R\rangle$

$$|\psi, t\rangle = \frac{1}{\sqrt{2}}\left(|+, t\rangle + |-, t\rangle\right) = \frac{1}{\sqrt{2}} e^{-i\epsilon_+ t}\left(|+\rangle + |-\rangle\, e^{-2i\Omega t}\right)$$

"spontaneous symmetry breaking"

Tabelle 1.

V/Q	T/τ	T
10	$2{,}4 \cdot 10^{4}$	$8 \cdot 10^{-10}$ sec
20	$3{,}8 \cdot 10^{8}$	10^{-5} sec
30	$6{,}9 \cdot 10^{12}$	0,2 sec
40	$1{,}3 \cdot 10^{17}$	1 Stunde
50	$2{,}9 \cdot 10^{21}$	3 Jahre
60	$5{,}2 \cdot 10^{25}$	$6 \cdot 10^{4}$ Jahre
70	$1{,}1 \cdot 10^{30}$	10^{9} Jahre

$$\Omega \approx \frac{3E_b}{\hbar} e^{-2\sqrt{2mE_b}\, a/\hbar}$$

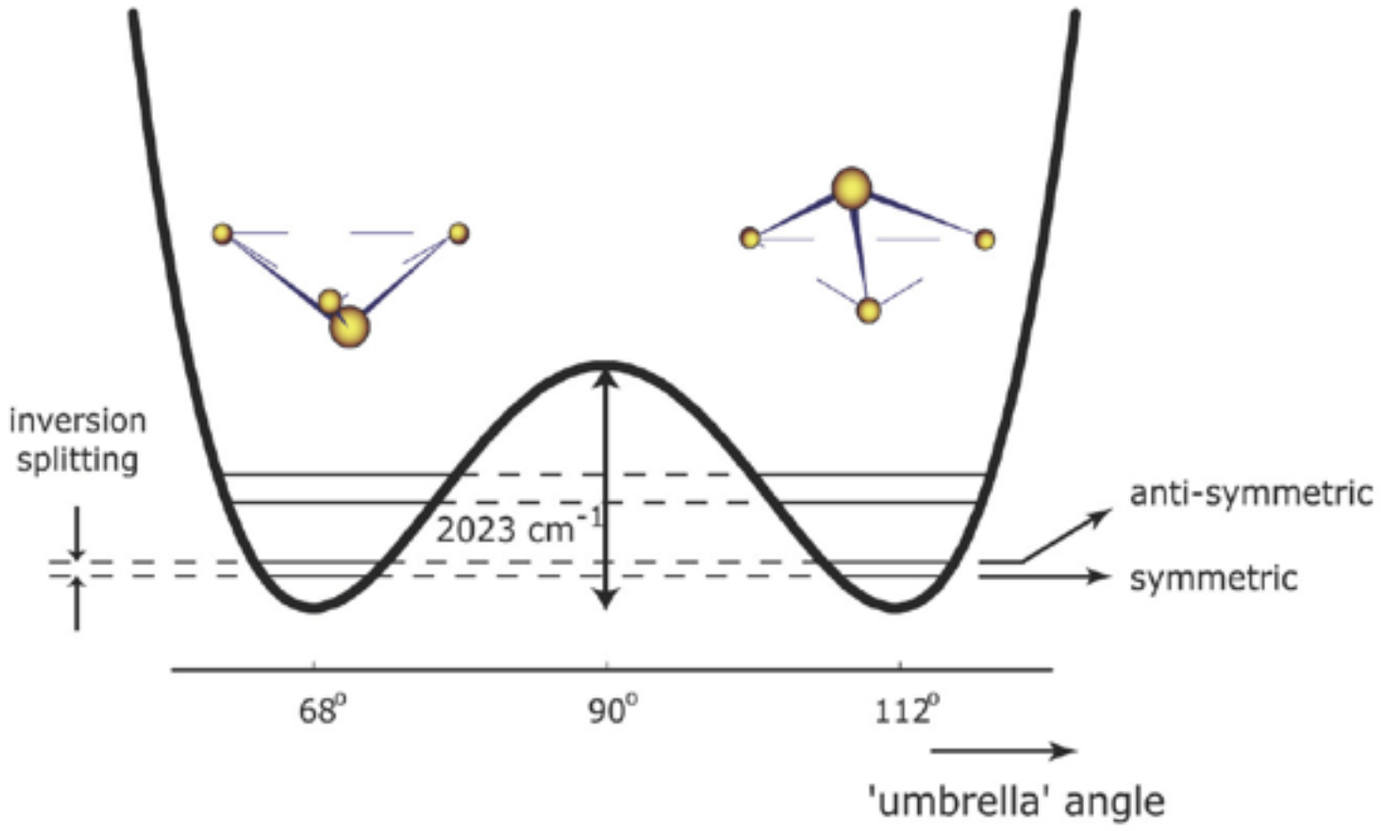

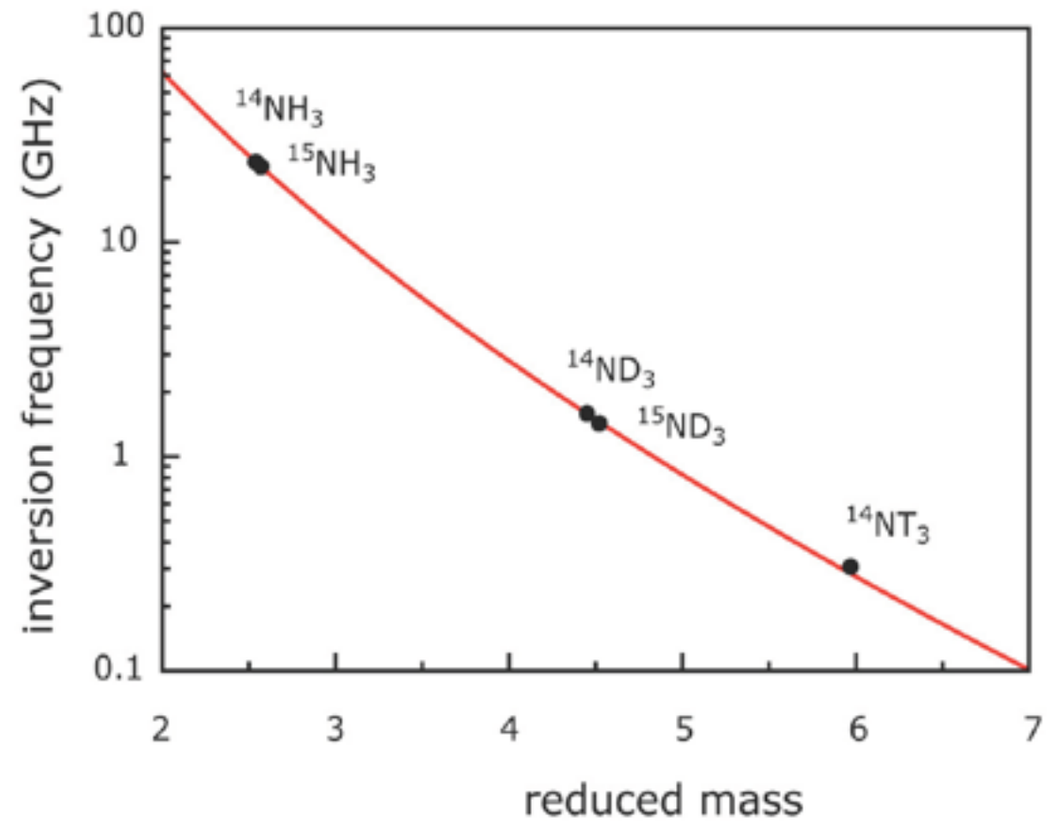

PF_3 no inversion

2nd paradox: why don't we observe the ground state?

Coupling to the environment: photons, gas atoms,...

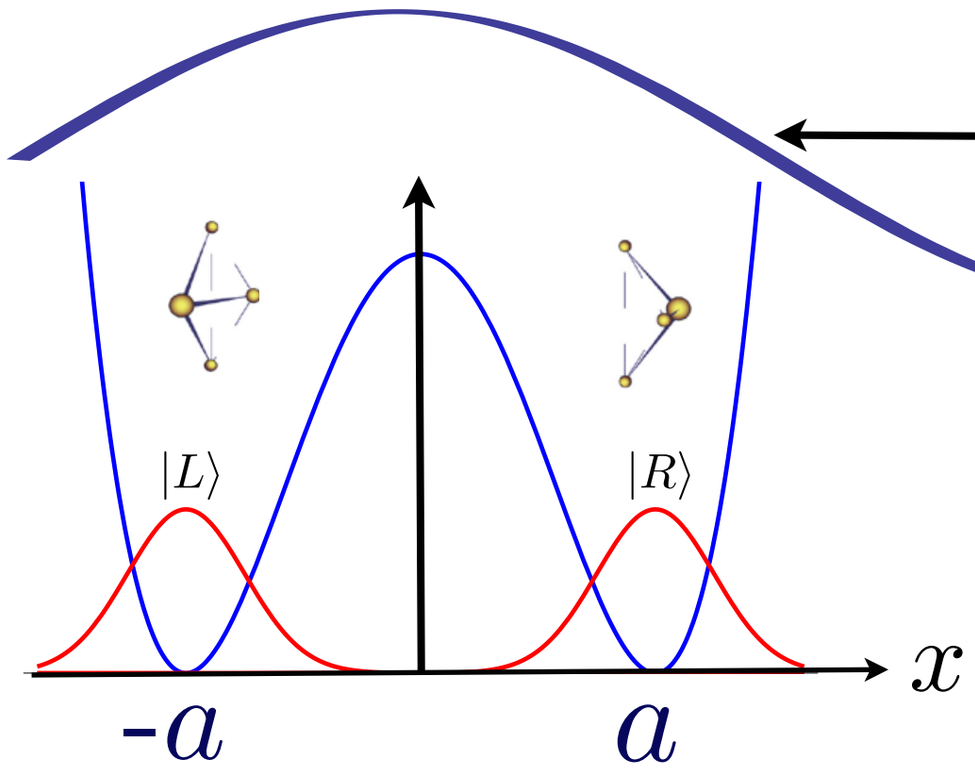

$$\phi(t) = \int_0^t dt' x(t') \dot{A}(x,t')$$

$$\dot{A}(x,t) = k \sum_i^{t/\tau} \delta(t - t_i) \cos(kx - \alpha_i)$$

$$\phi_R - \phi_L = 2 \sum_i^{t/\tau} \cos\alpha_i \cos(ka)$$

$$\left\langle (\phi_R(t) - \phi_L(t))^2 \right\rangle^{1/2} = 2\pi t \lambda_{dec} \qquad \lambda_{dec} = \frac{[\sin(ka)]^2}{2\pi\tau}$$

thermal photons $\qquad \lambda_{dec} \sim a^2 \sigma c \left(\frac{k_B T}{\hbar c}\right)^5$

Time evolution: description by density matrix

$$\rho = \frac{1}{2}\left(\mathbf{1} + \rho_y \hat{\boldsymbol{\sigma}}_y + \rho_z \hat{\boldsymbol{\sigma}}_z\right), \quad \rho_y = i\rho_{RL} - i\rho_{LR} \quad \rho_z = \rho_{LL} - \rho_{RR}$$

$$\rho_{RL} \to \rho_{RL} e^{i(\phi_R - \phi_L)} \to \rho_{RL} e^{-\left\langle (\phi_R - \phi_L)^2 \right\rangle / 2}$$

$$i\dot{\rho} = [\hat{\mathcal{H}}, \rho] \qquad \dot{\rho}_y = -\lambda_{dec}\rho_y - \Omega\rho_z$$
$$\dot{\rho}_z = \Omega\rho_y$$

Harris and Stodolsky 1982

$$\rho_z(t) = \rho_z(0)\left(\frac{\Omega^2}{\lambda_{dec}} e^{-\lambda_{dec} t} + e^{-(\Omega^2/\lambda_{dec})t}\right) \qquad \Omega \ll \lambda_{dec}$$

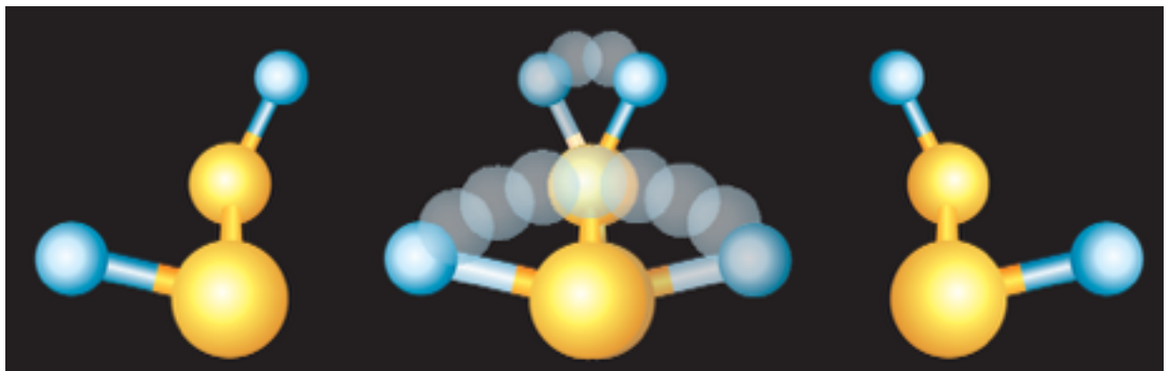

Figure 1. Dideuterium disulfide exists in left-handed (left) and right-handed (right) forms, thanks to its spatial arrangement of deuterium atoms (blue) and sulfur atoms (yellow). In principle, D_2S_2 can also exist in a superposition of the two isomers (middle). (Adapted from I. Thanopulos, P. Král, M. Shapiro, *J. Chem. Phys.* **119**, 5105, 2003.)

Trost and Hornberger (2009) D_2S_2 in He:

$$\Omega \approx 176 \text{ s}^{-1}, \qquad \lambda_{dec} \approx 9 \times 10^9 \text{ s}^{-1}$$

Motivation

JOURNAL OF APPLIED PHYSICS VOLUME 95, NUMBER 11 1 JUNE 2004

Imaging spiral magnetic domains in Ho metal using circularly polarized Bragg diffraction

J. C. Lang, D. R. Lee, D. Haskel, and G. Srajer
Advanced Photon Source, Argonne National Laboratory, Argonne, Illinois 60439

(Presented on 6 January 2004)

We have used circularly polarized x rays to image the spiral magnetic domain structure in a single crystal of Ho metal. In these structures, the magnetization direction rotates between successive atomic layers forming a helix. At magnetic Bragg diffraction peaks, circularly polarized x rays are sensitive to the handedness of such a helix (i.e., either right or left handed). By reversing the helicity of the incident beam with phase-retarding optics and measuring the difference in the Bragg scattering, contrast between domains of opposing handedness can be obtained. © *2004 American Institute of Physics*. [DOI: 10.1063/1.1688252]

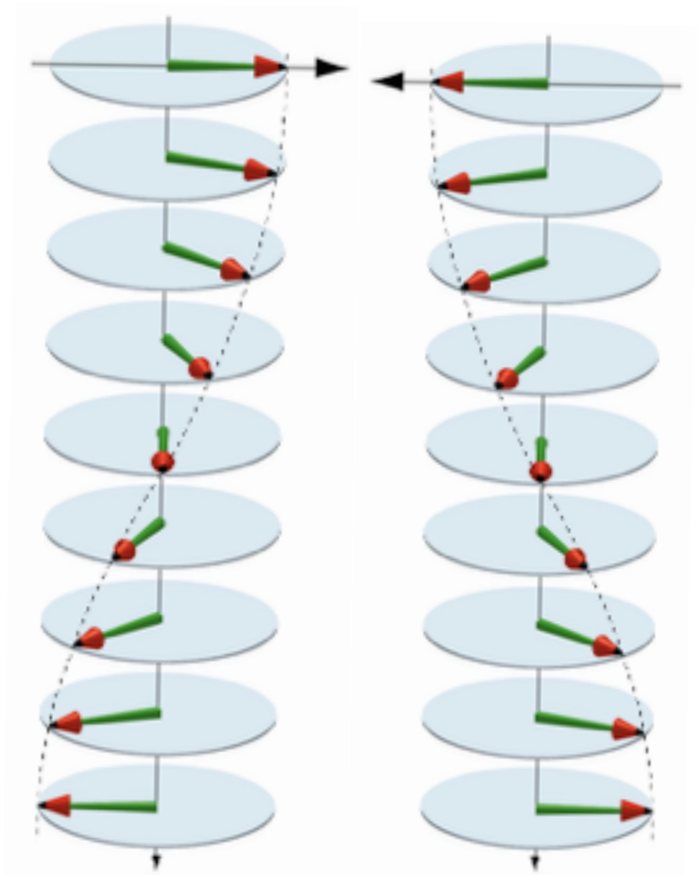

film plane perpendicular to helical axis

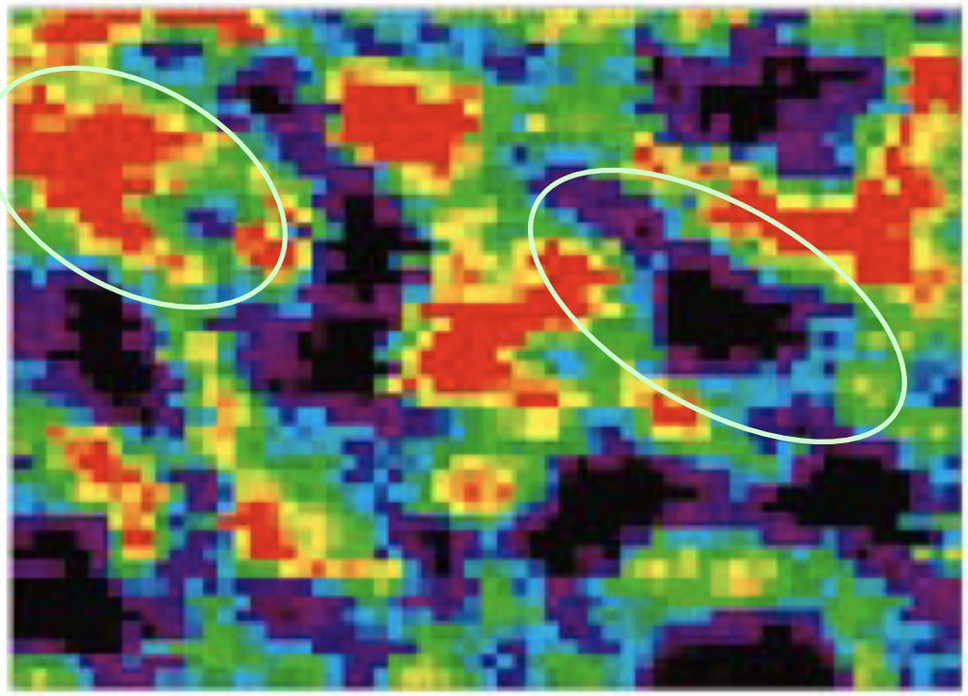

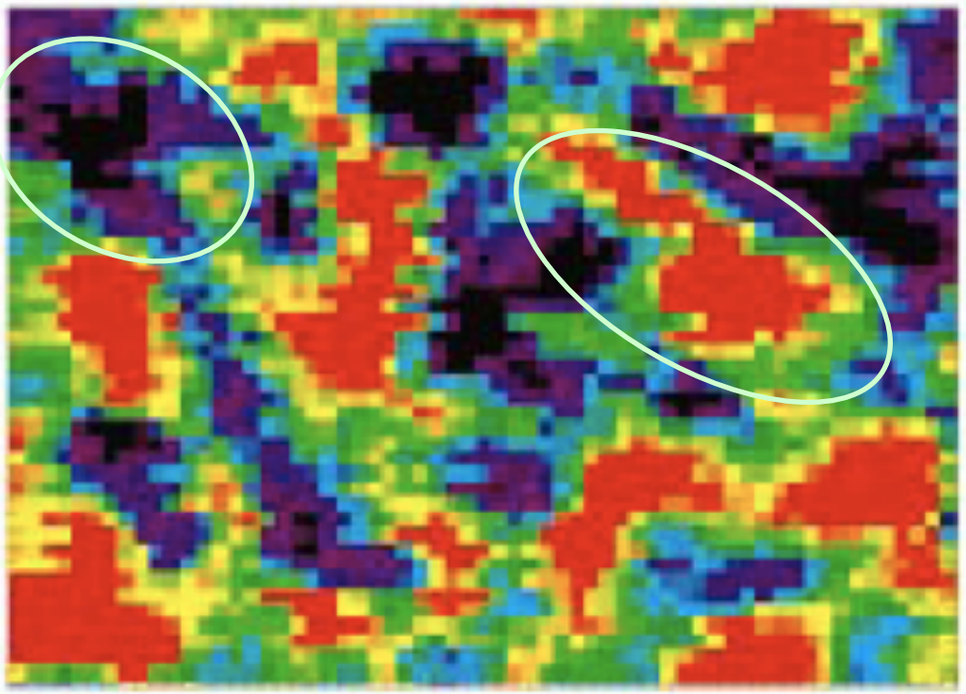

$450\mu m$

Motivation

How do the domain walls look like?

Neel wall

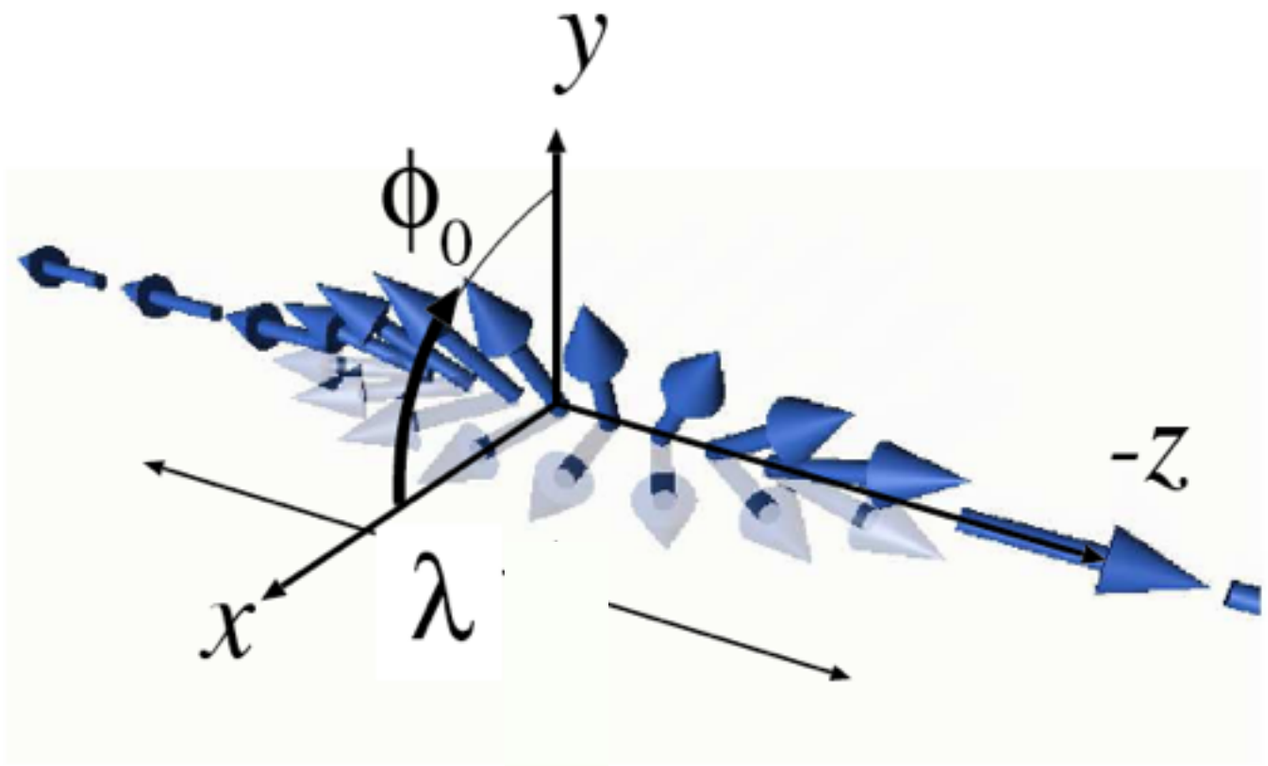

Bloch wall (Bloch 1932)

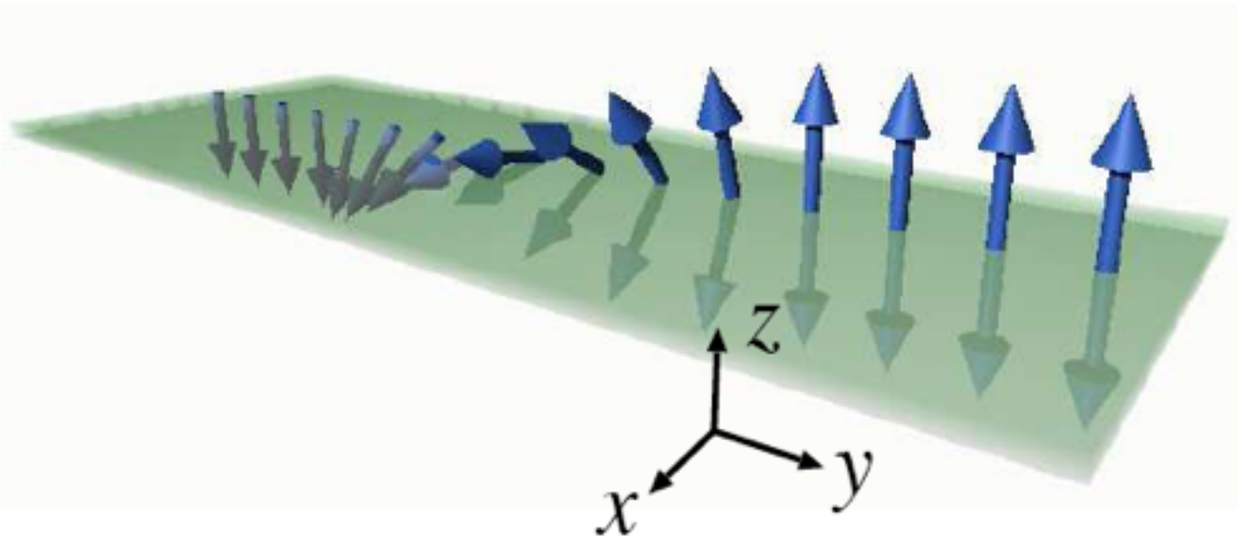

Time reveral symmetry

Time reversal transformation:

$$\hat{T}\,\mathbf{t} = -\mathbf{t}$$

$$\hat{T}\,\mathbf{E} = \mathbf{E}$$

$$\hat{T}\,\mathbf{B} = -\mathbf{B}$$

$$\boldsymbol{\nabla} E = \rho$$

$$\boldsymbol{\nabla} B = 0$$

$$\boldsymbol{\nabla} \times \mathbf{E} = \frac{1}{c}\dot{\boldsymbol{B}}$$

$$\boldsymbol{\nabla} \times \mathbf{B} = \frac{1}{c}\boldsymbol{j} + \frac{1}{c}\dot{\boldsymbol{E}}$$

$$m\ddot{\mathbf{r}} = e\boldsymbol{E} + \frac{e}{c}\dot{\boldsymbol{r}} \times \boldsymbol{B}$$

JOURNAL OF THE PHYSICAL SOCIETY OF JAPAN, Vol. 14, No. 6, JUNE, 1959

A New Type of Antiferromagnetic Structure in the Rutile Type Crystal

By Akio YOSHIMORI

Department of Physics, University of Osaka Prefecture, Mozu-Higashi, Sakai

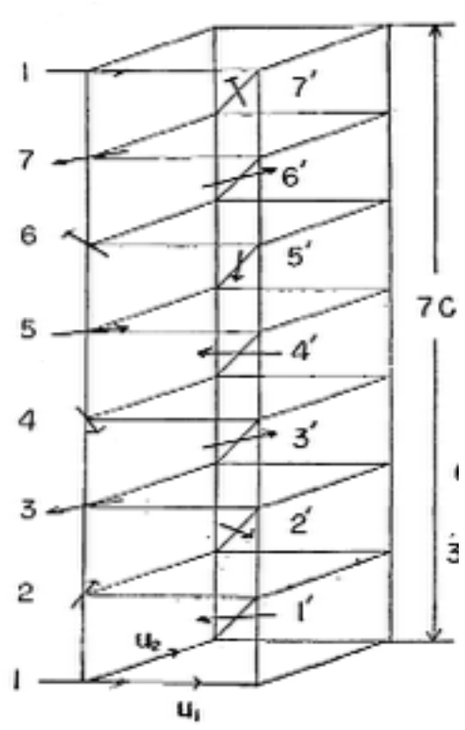

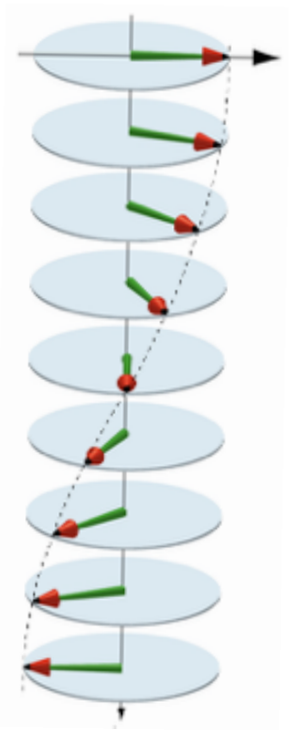

Chiral Magnets: time reversal + spatial inversion symmetry broken

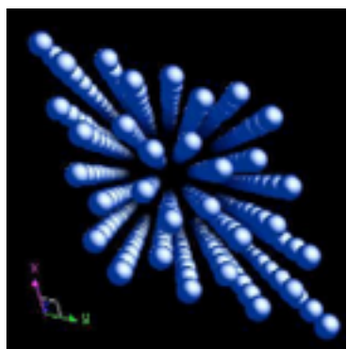

simultaneously

separately

centrosymmetric crystals: space group contains inversion center

non-centrosymmetric crystals: space group contains no inversion center

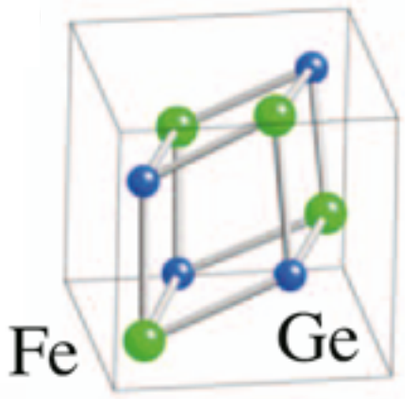

Centrosymmetric Crystals

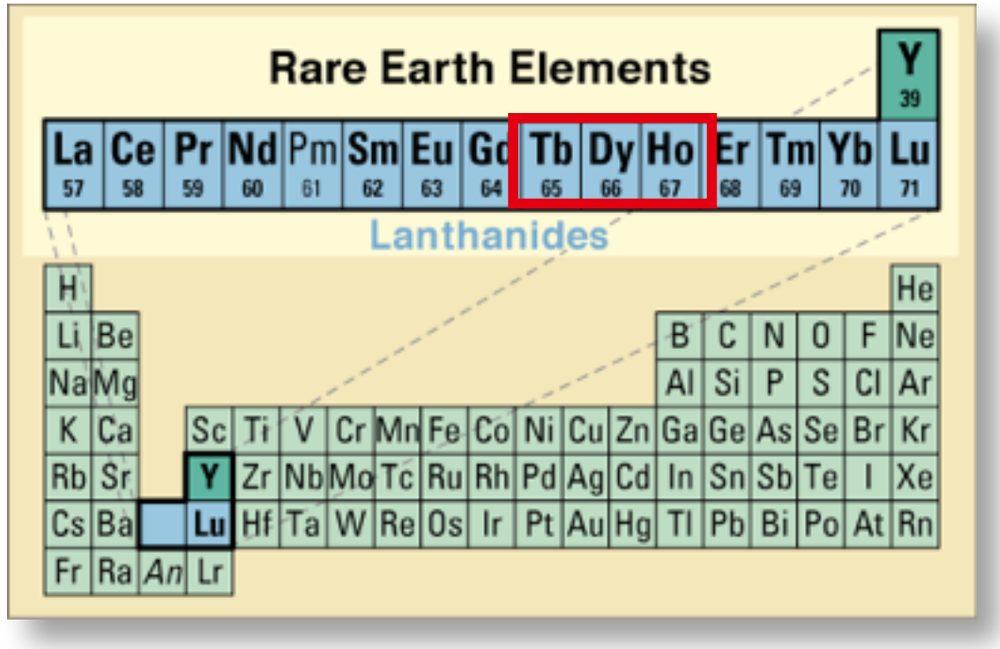

Tb, Dy, Ho :
RKKY interaction →
frustration → helical structure

$RMnO_3$ $R \in \{Y, Tb, Dy\}$

$R_2Mn_2O_5$, $R \in \{Tb, Bi\}$

$Ni_3V_2O_8$ and $LiCu_2O_2$

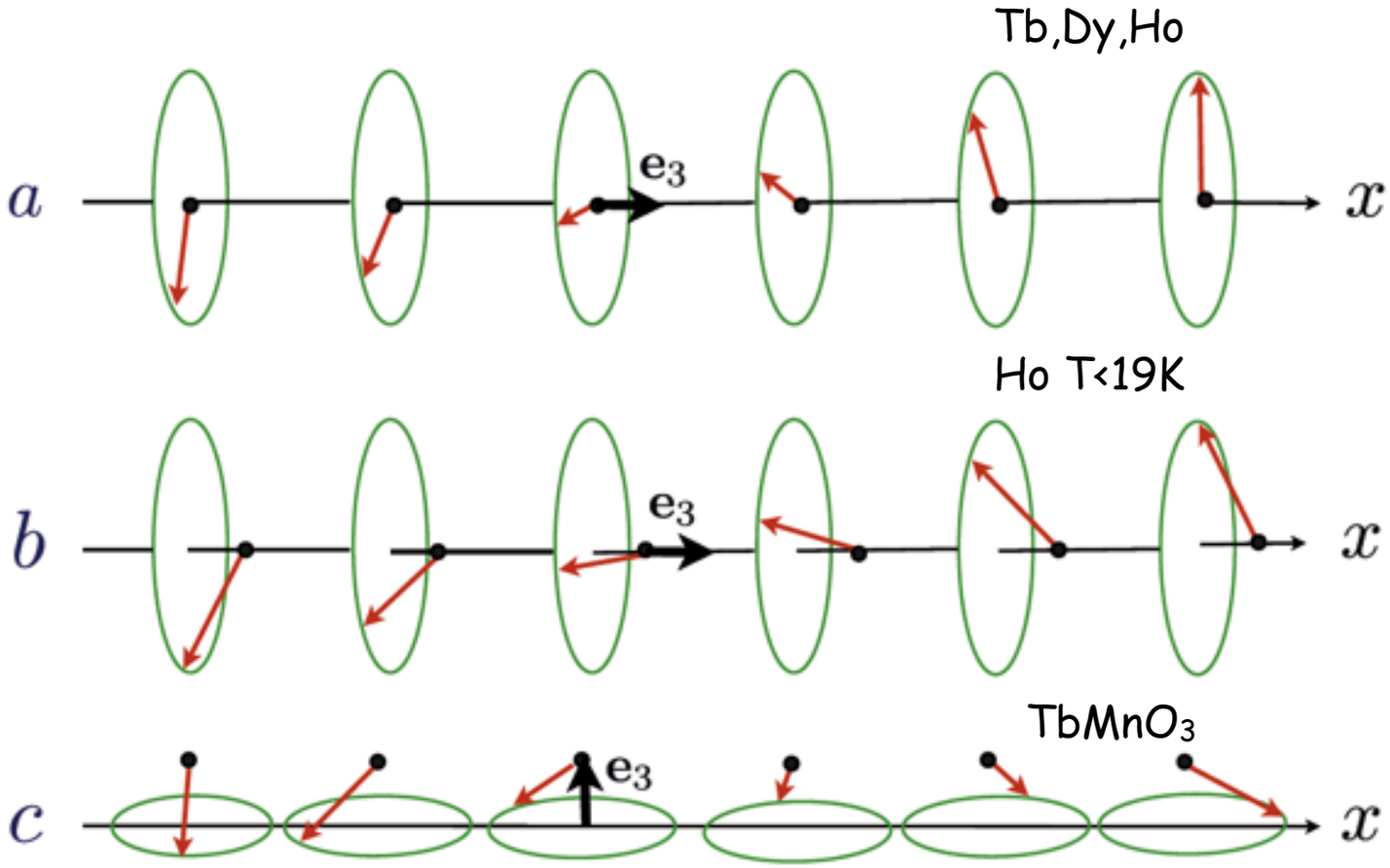

both right-handed and left-handed helices appear!

Centrosymmetric Crystals: Model

$$\mathbf{r} \to -\mathbf{r} \quad t \to -t$$

$$\theta = qa \ll 1$$

$$\mathcal{H} = \frac{J}{a}\int_r \Big\{ -\frac{\theta^2}{2}(\partial_x \mathbf{m}_\perp)^2 + \frac{a^2}{4}(\partial_x^2 \mathbf{m}_\perp)^2 + (\nabla_\perp \mathbf{m})^2 + (\partial_x m_3)^2 + V(m_3)\Big\}.$$

$$\mathbf{m} = |m_\perp|\,(\mathbf{e}_1 \cos qx + \chi \mathbf{e}_2 \sin qx) + \zeta |m_3| \mathbf{e}_3$$

$\chi = \pm 1$ *chirality*

$\zeta = \pm 1$ *conicity*

$$\mathbf{m} = \mathbf{m}(\vartheta, \varphi)$$

$$\mathcal{H} = \frac{J}{2}\int d^3r \left\{ \varphi_\perp^2 + \frac{1}{4}(\varphi_x - \theta)^2(\varphi_x + \theta)^2 + \frac{1}{4}\varphi_{xx}^2 \right\}$$

$$\mathcal{H} = \frac{J}{2}\int d^3r \left\{ \varphi_\perp^2 + \theta^2[\varphi_x - A(\mathbf{r})]^2 + \frac{1}{4}\varphi_{xx}^2 \right\}$$

$A = \theta$

$A = -\theta$

JOURNAL DE PHYSIQUE *Colloque* C6, *supplément au n°* 8, *Tome* 39, *août* 1978, *page* C6-1450

SOLITONS IN LOW TEMPERATURE PHYSICS

K. Maki

Department of Physics University of Southern California,Los Angeles, California 90007, U.S.A.

Résumé.- Les solitons sont des solutions spéciales des équations nonlinéaires. Ils sont des objets localisés qui se comportent comme des corpuscules classiques. Les solitons paraissent jouer un rôle de plus en plus important dans la physique des basses températures.

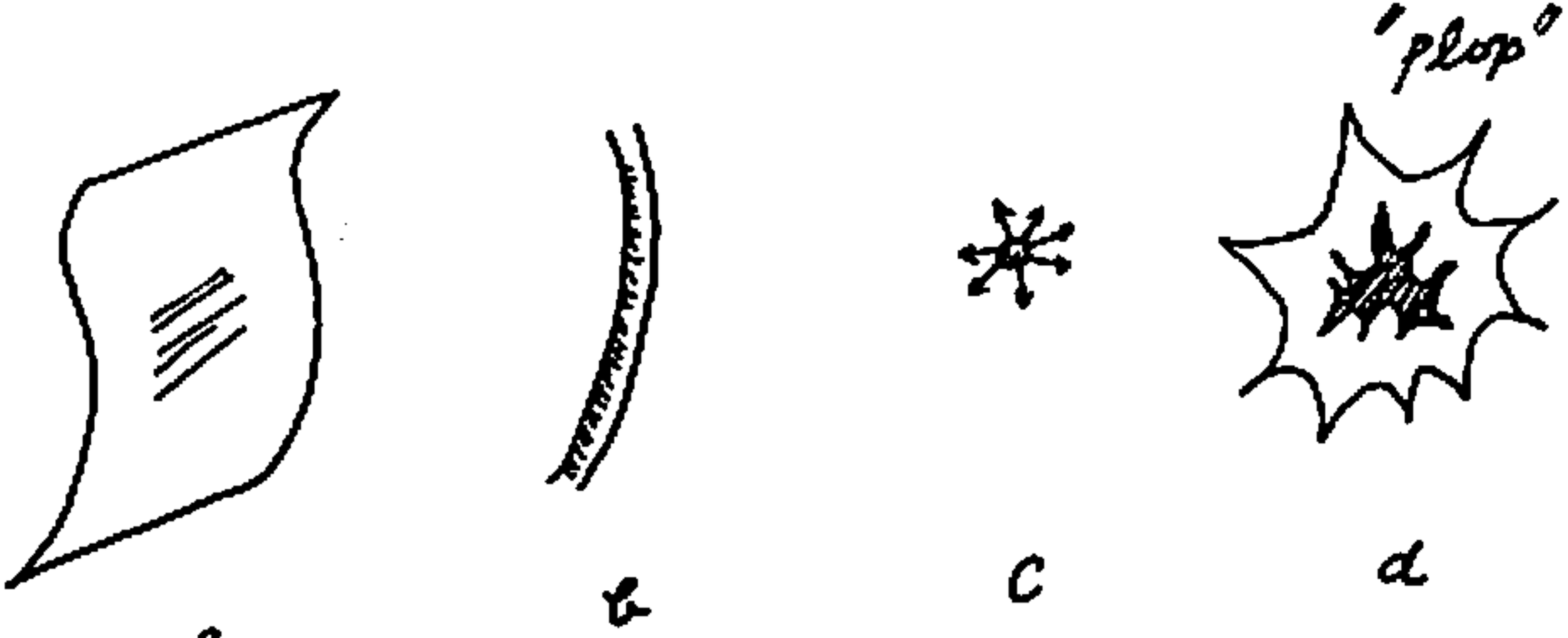

Classification of defect structures according to homotopy groups :

Toulouse & Kleman (1976)
Volovik & Mineev (1977)
Mermin (1979)

Degeneracy space $\mathcal{R}$

Consider mapping of a subspace $\mathcal{V}_d$ of $\mathbb{R}^3$ on $\mathcal{R}$

Ensemble of equivalent mappings: homotopy group $\pi_d(\mathcal{R})$

Example: Ising domain wall,

$$\pi_0(\mathcal{R}) = Z_2$$

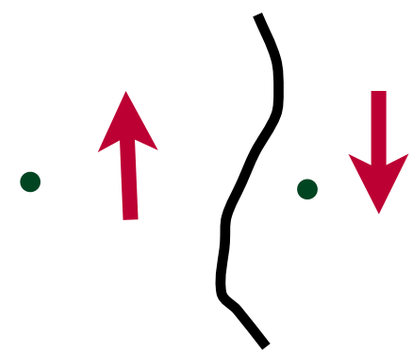

Defects: vortex line perpendicular and parallel to helix

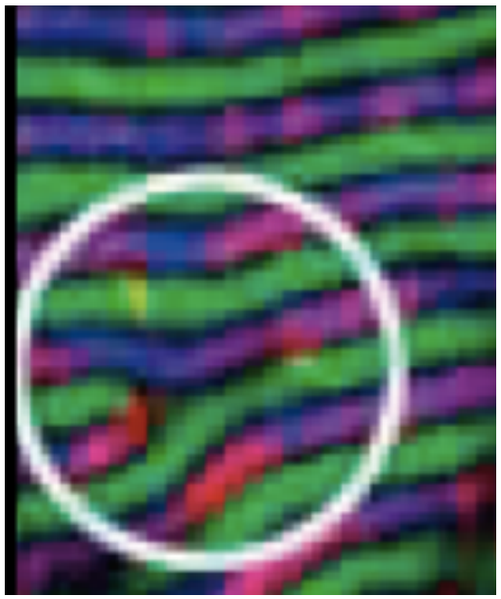

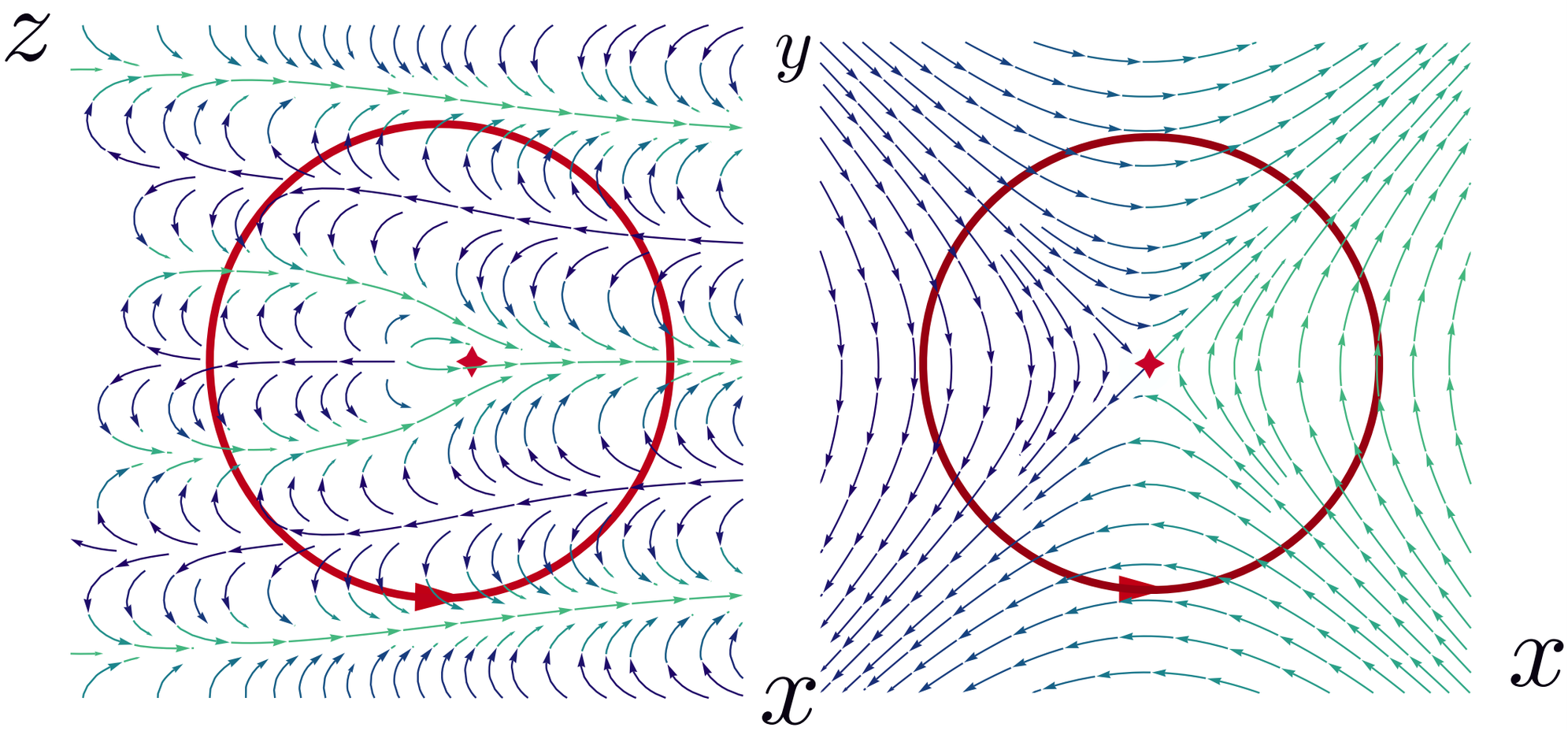

FeGe, Tokura et al. ,08

$$n_w = \oint_C d\varphi/2\pi = -1$$

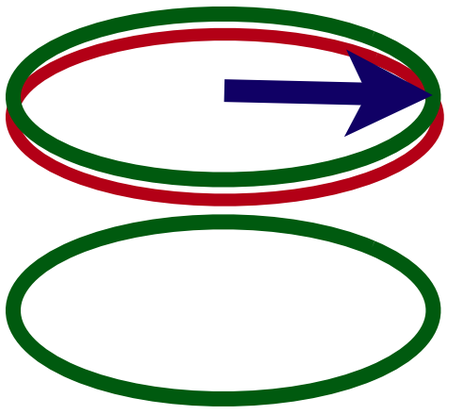

degeneracy space

$$\mathcal{R} = \mathcal{S}^1 \times \mathcal{S}^0$$

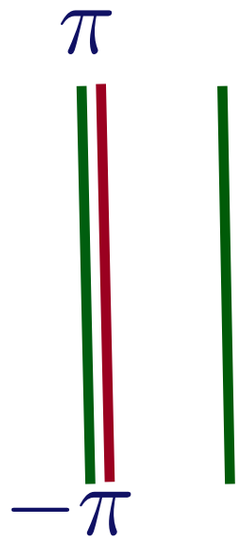

$$\oint d\varphi = 2\pi$$

?

Very different from Bloch or Neel walls!

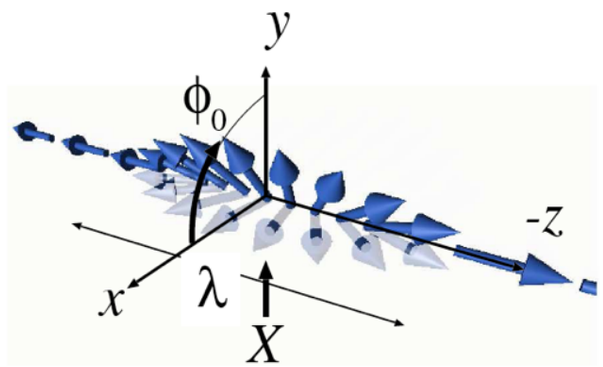

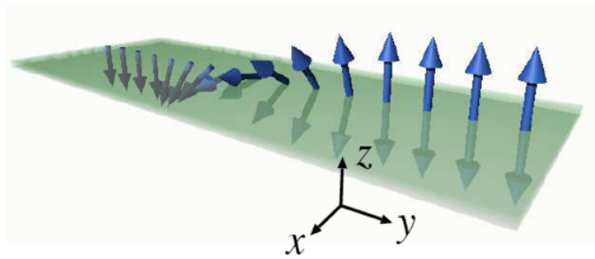

Defects: domain walls

Hubert walls
perpendicular to helix

Vortex domain wall
parallel to helix

path in real space

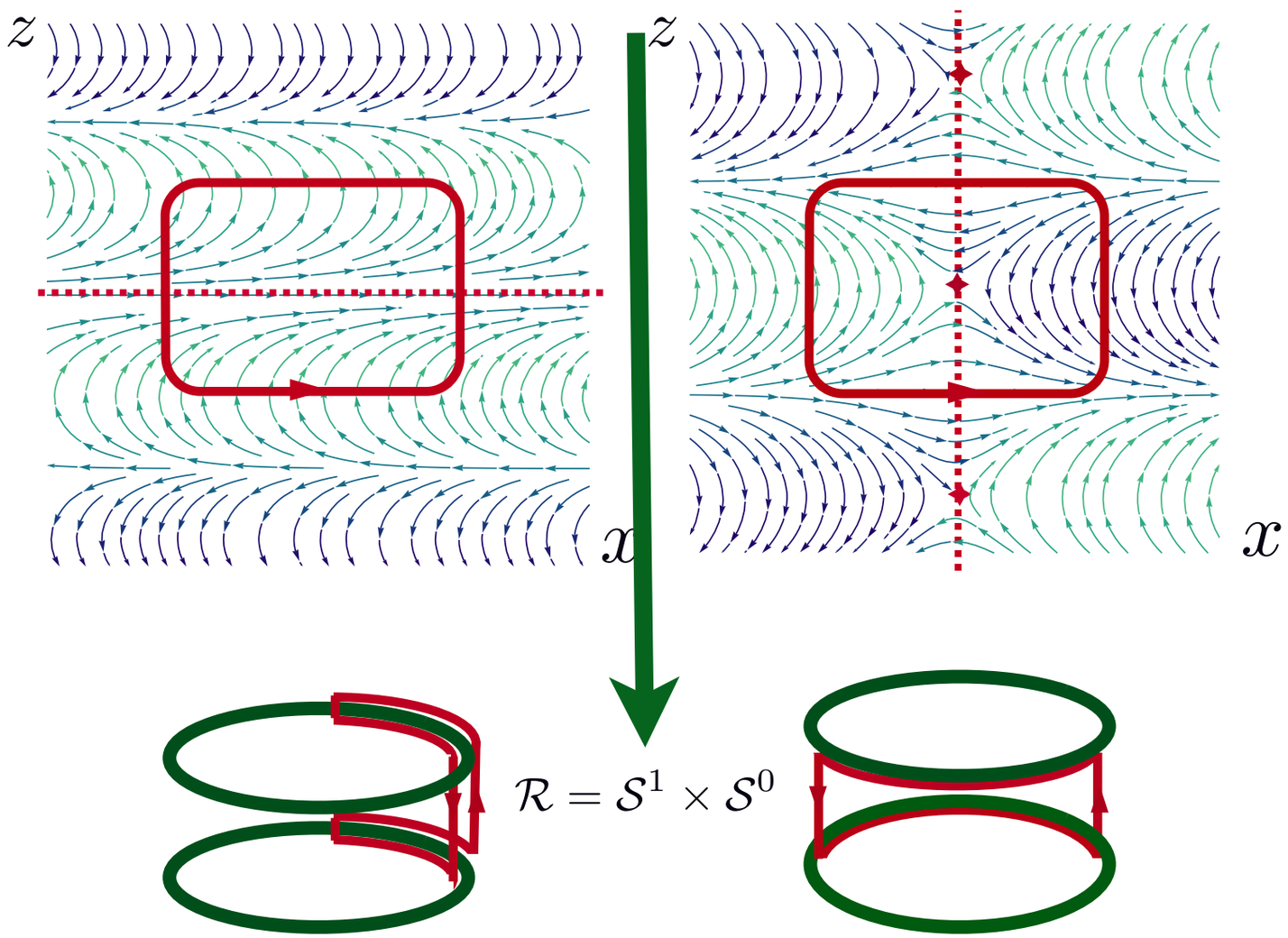

$\mathcal{R} = \mathcal{S}^1 \times \mathcal{S}^0$

path in degeneracy space

$CuCrO_2$

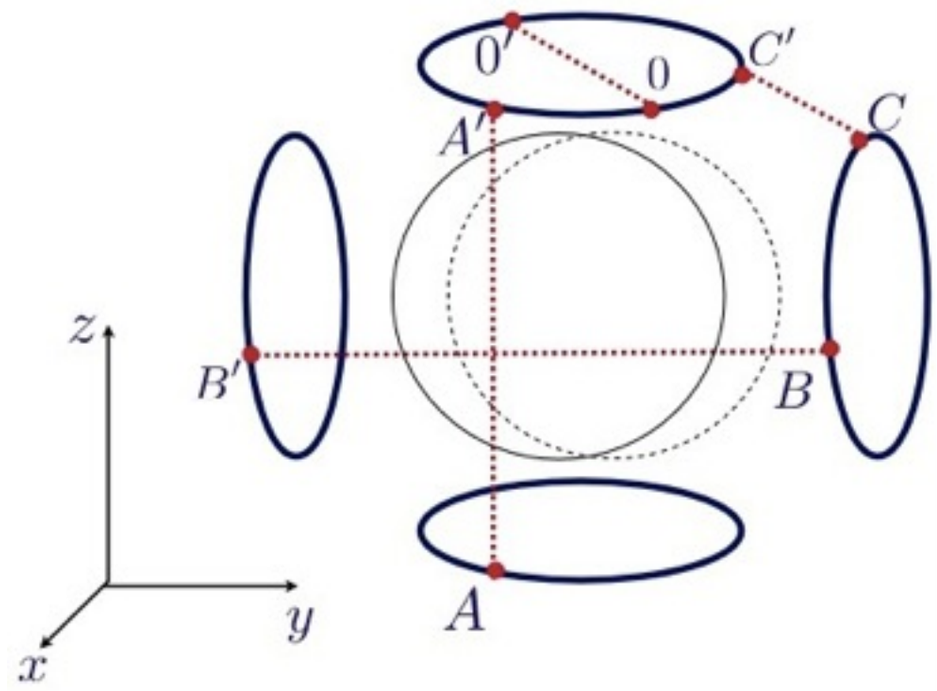

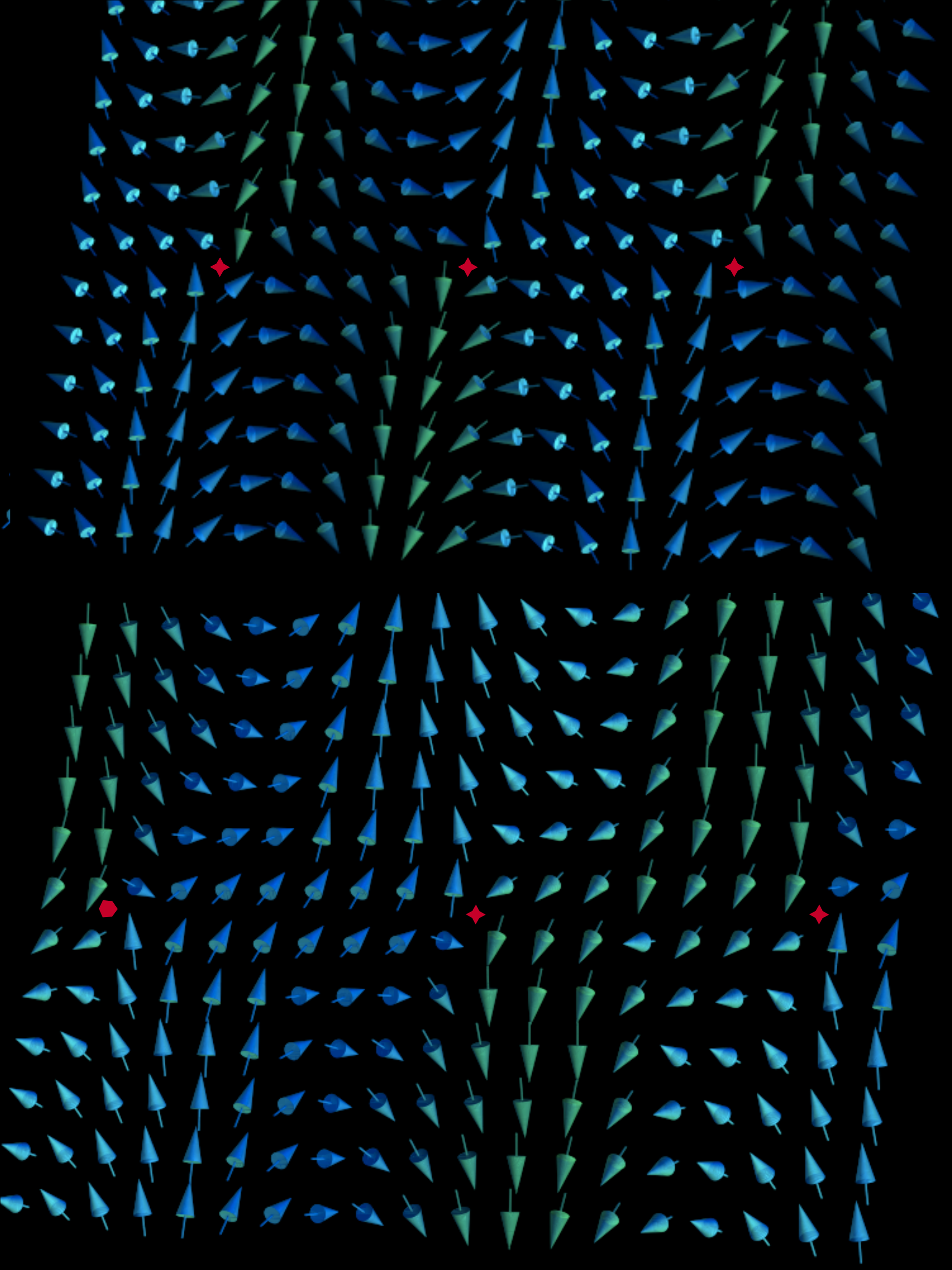

Centrosymmetric Crystals: Topological Hall effect*

*Ye, Kim, Millis, Shraiman, Majumdar, and Tesanovic

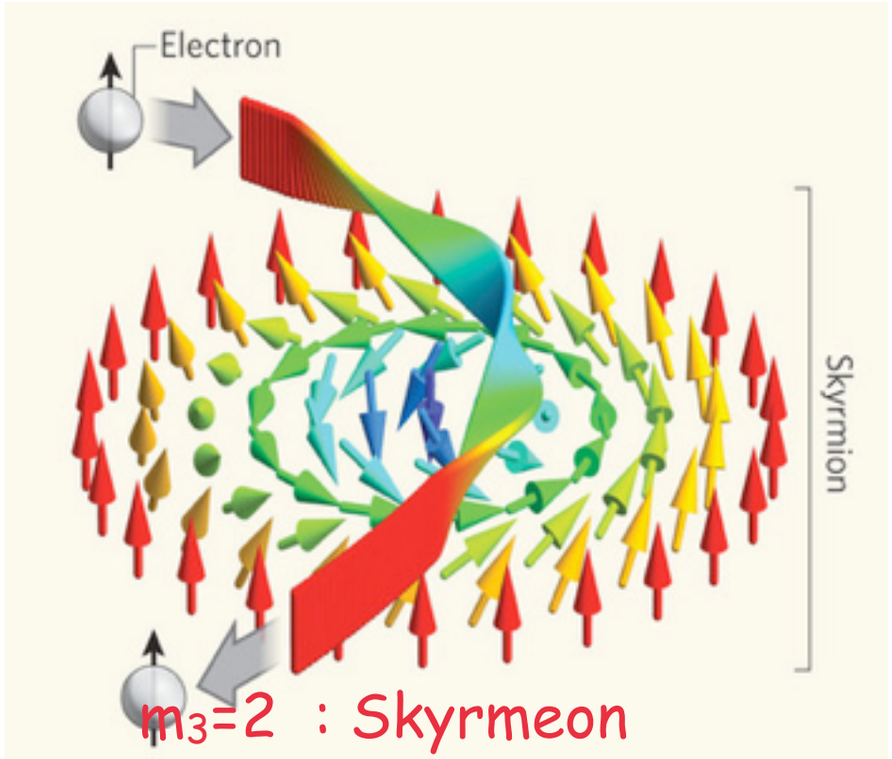

Electrons moving adiabatically in exchange field of magnetization experience Berry's magnetic field

$$B_\alpha = \frac{\phi_0}{8\pi}\epsilon_{\alpha\beta\gamma}\mathbf{m}\cdot(\partial_\beta\mathbf{m}\times\partial_\gamma\mathbf{m})$$

$$\phi_B = \frac{\phi_0}{4\pi}\int d\cos\vartheta d\varphi = \frac{\phi_0}{2}m_3.$$

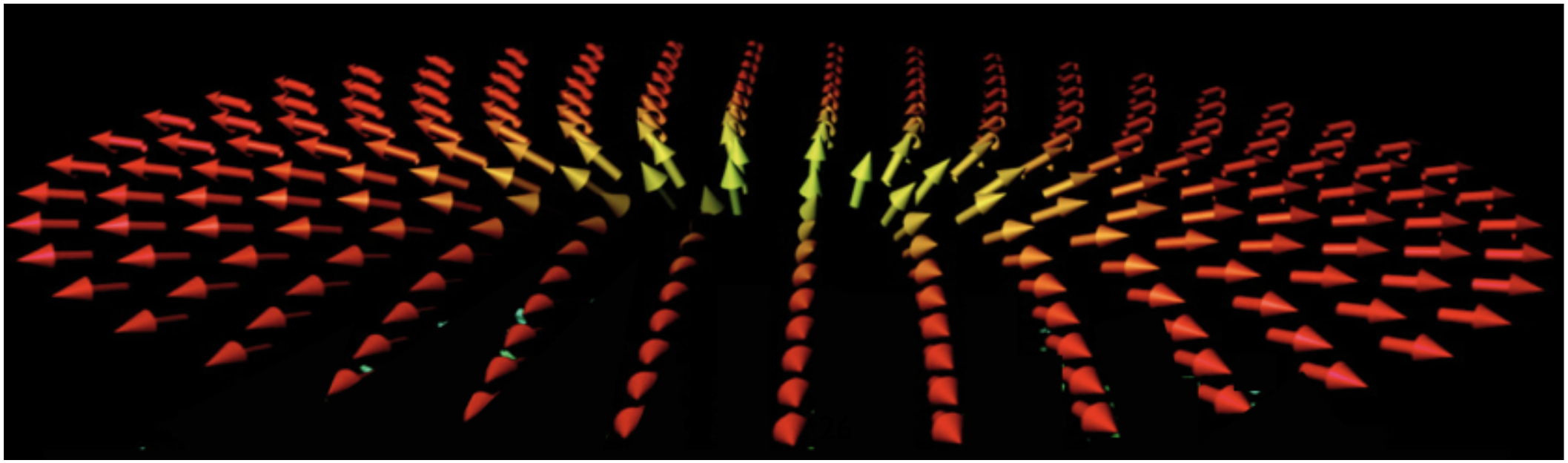

Centrosymmetric Crystals: Topological Hall effect*

force on vortex line

$$\mathbf{f} = \tfrac{1}{c}\mathbf{j} \times \mathbf{e}_3 \phi_B \ .$$

$$p = m_3 \theta \frac{j}{10^5\, A m^{-2}}\, N m^{-2}$$

$$p_c = J \theta n_i a/6 \approx \theta \frac{T_c}{20K}\, \frac{n_i}{10^{17} cm^{-3}}\, N m^{-2}$$

$$j_c \approx 6 \cdot 10^7\, A m^{-2}$$

m_3=1 : Meron

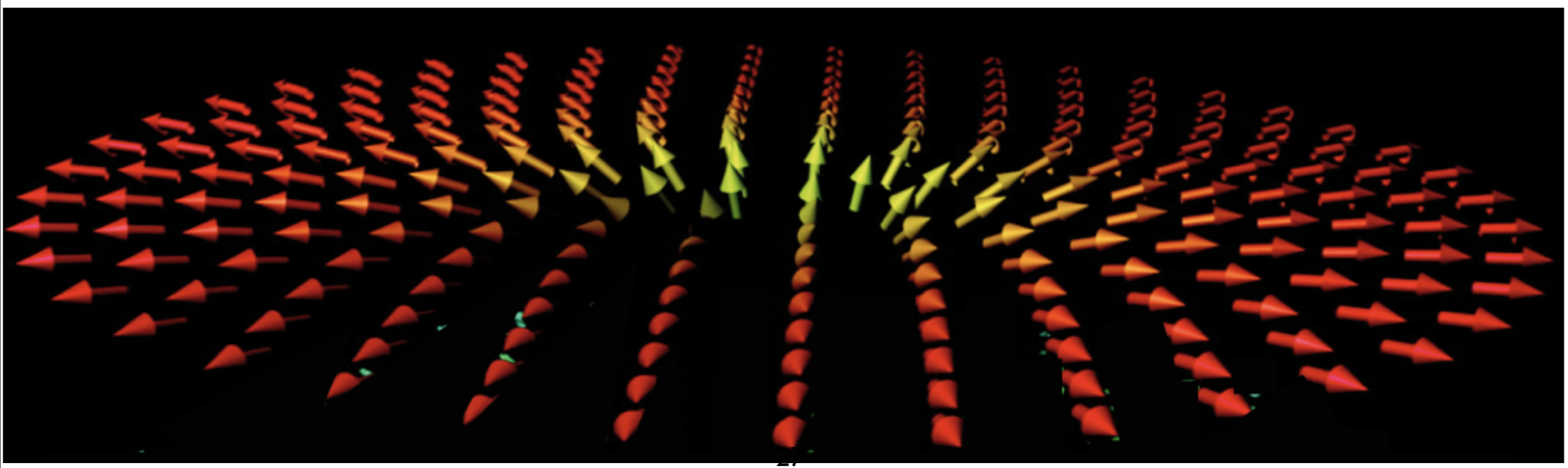

Centrosymmetric Crystals: Multiferroics

Coupling to electric polarization $\mathbf{P} = \kappa \left[\mathbf{m}(\nabla \cdot \mathbf{m}) - (\mathbf{m} \cdot \nabla)\mathbf{m}\right]$

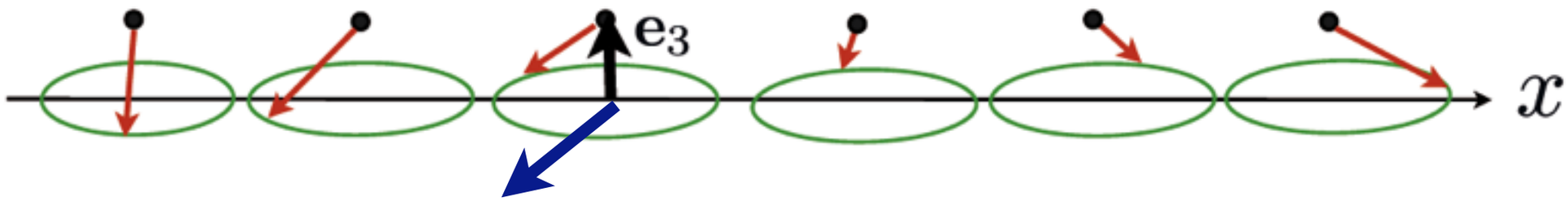

vortex lines are charged

$$\rho^{(1)} = 2\pi n_w \kappa \left[\mathbf{e}_3 \times \hat{x}\right] \hat{\mathbf{n}}$$

Wall in yz-plane similar to Neel wall: magnetization rotates around axis in the wall

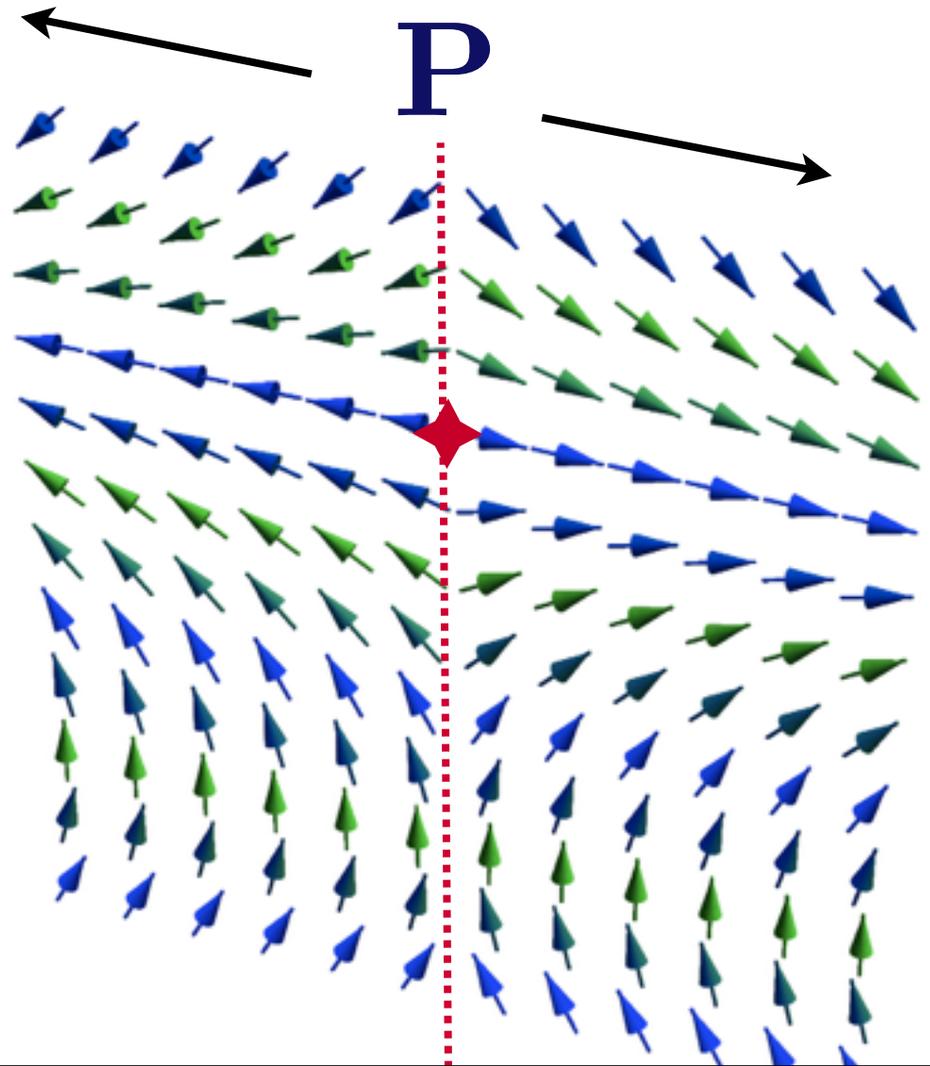

Centrosymmetric Crystals: Domain

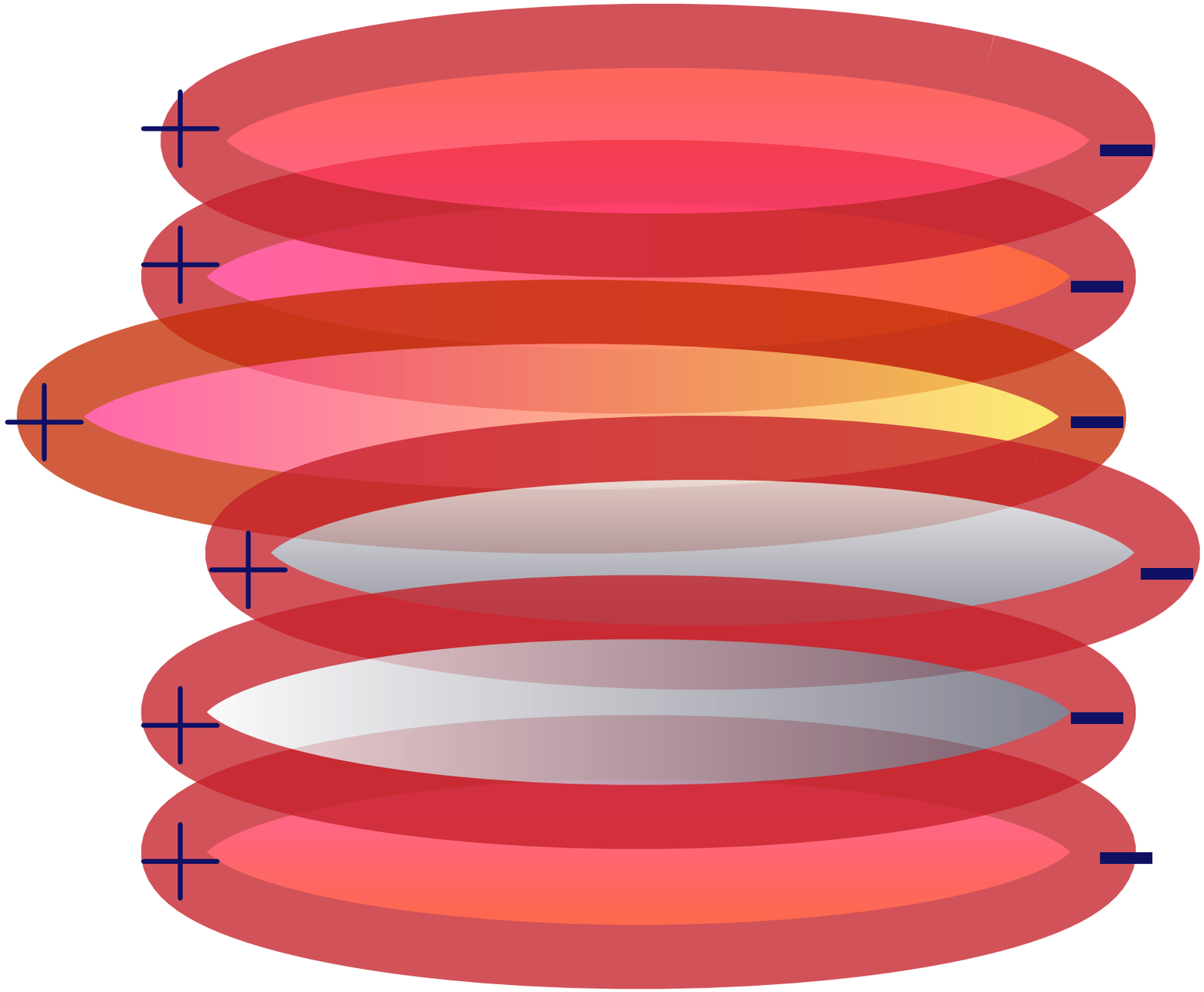

Non-Centrosymmetric Crystals: systems and model

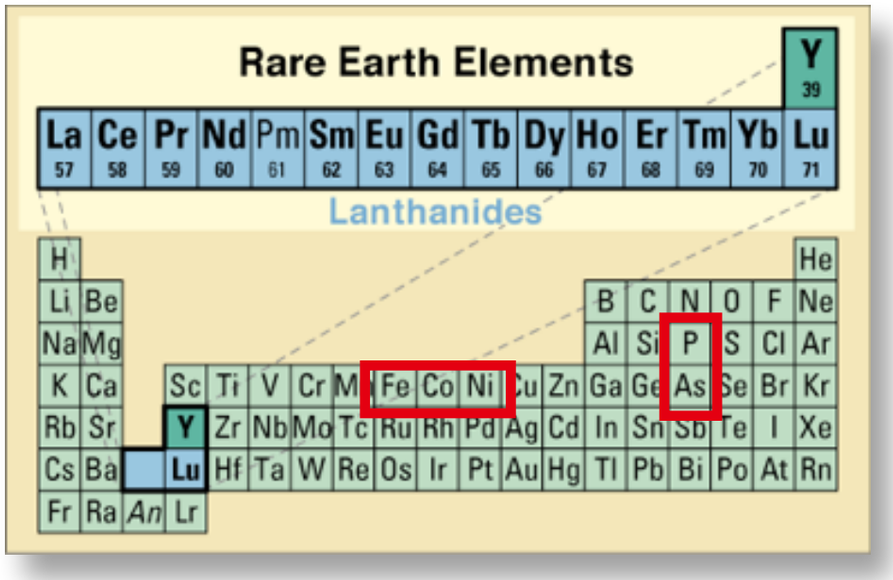

FeGe , MnSi, $Fe_{1-x}Co_xSi$

Heisenberg-spins + weak cubic anisotropy

Dzyaloshinskii-Moriya interaction $g\mathbf{M}_i \times \mathbf{M}_j$

$$\mathcal{H}_{ncs} = J/a \int d^3r \left\{ (\boldsymbol{\nabla} \boldsymbol{m})^2 + 2q\, \boldsymbol{m} \cdot [\boldsymbol{\nabla} \times \boldsymbol{m}] + v \sum_\alpha m_\alpha^4 \right\}$$

$$v = O(q^4) \qquad \boldsymbol{m}(\boldsymbol{r}) = \mathbf{e}_1 \cos\varphi(\boldsymbol{r}) + q^{-1} \boldsymbol{\nabla}\varphi \times \mathbf{e}_1 \sin\varphi(\boldsymbol{r}),$$

$\mathcal{R} = SO(3)/Z_2$

$\pi_3(\mathcal{R}) = Z$ (non-trivial texture)
$\pi_2(\mathcal{R}) = 0$ (no point defects)
$\pi_1(\mathcal{R}) = Z_4$ (stable line defects)

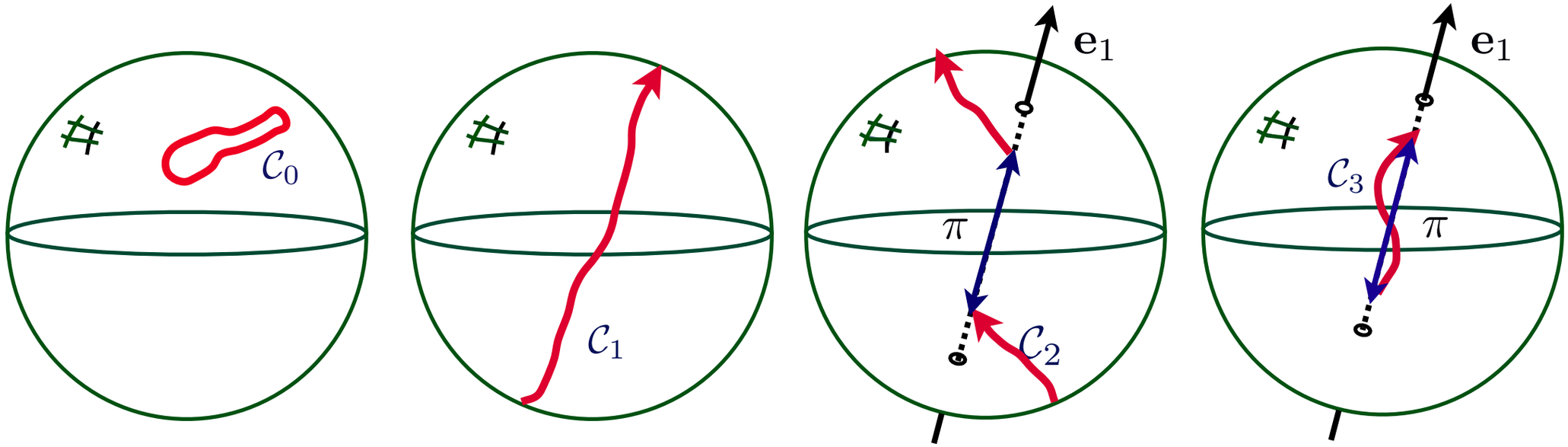

G.E. Volovik, V.P. Mineev, 1977, "Investigation of singularities in superuid 3He and liquid crystals by homotopic topology methods," Sov.Phys. JETP 45 1186 - 1196

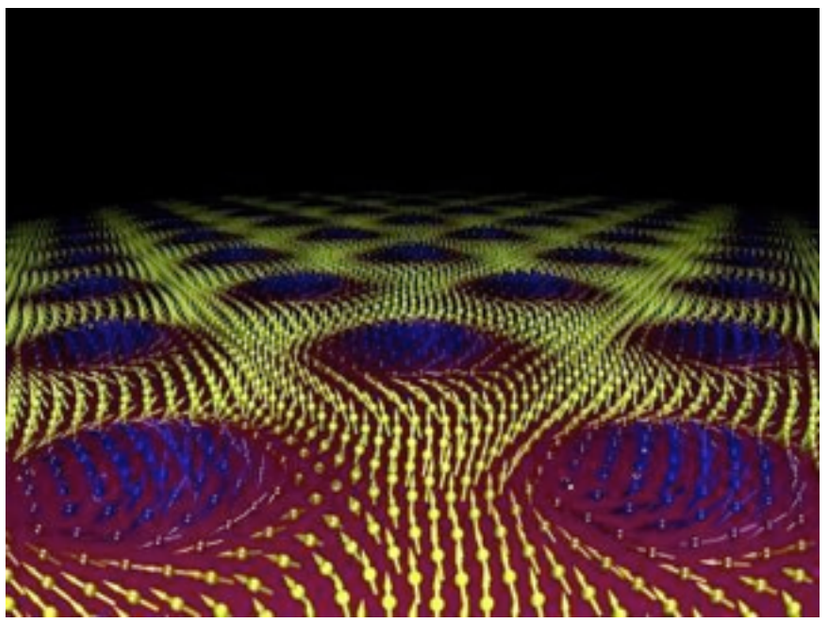

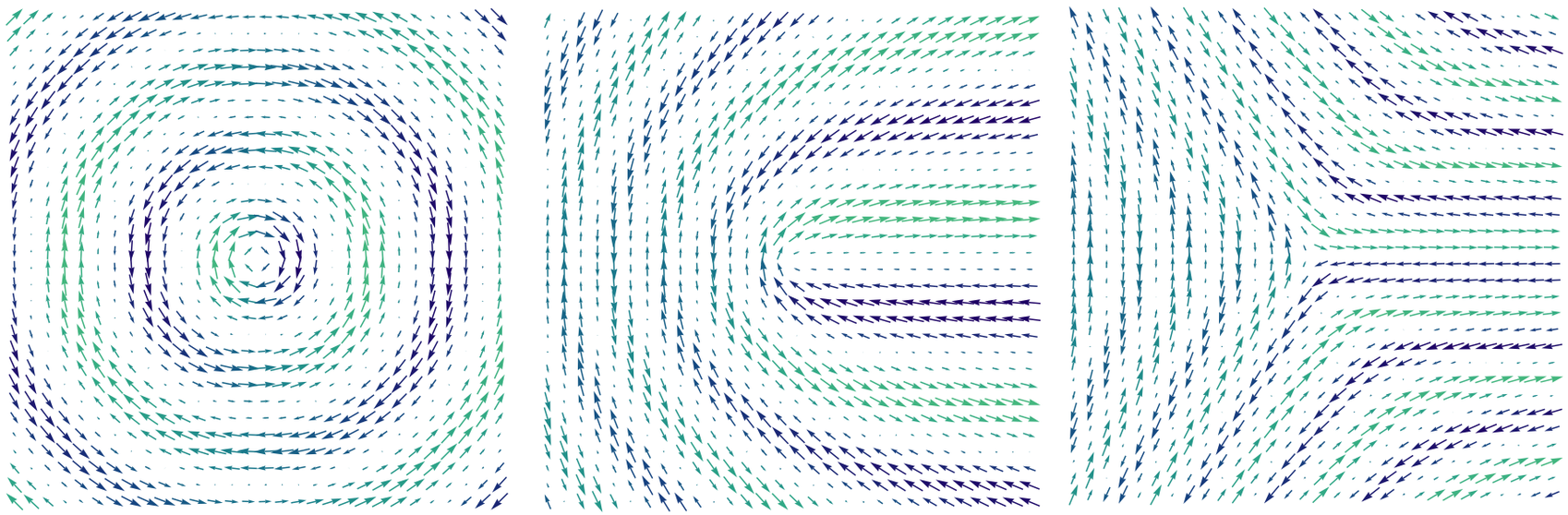

2π-disclination

π-disclination

-π-disclination

Non-Centrosymmetric Crystals: Hubert walls

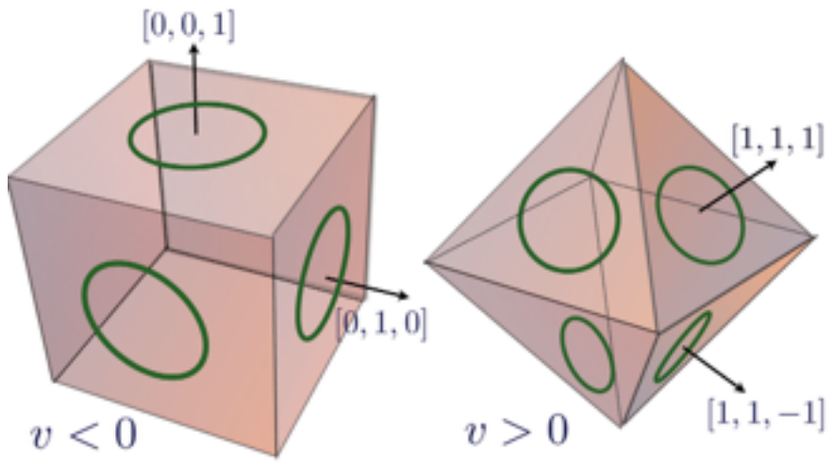

Domain wall bisector to
wave vectors of adjacent domains

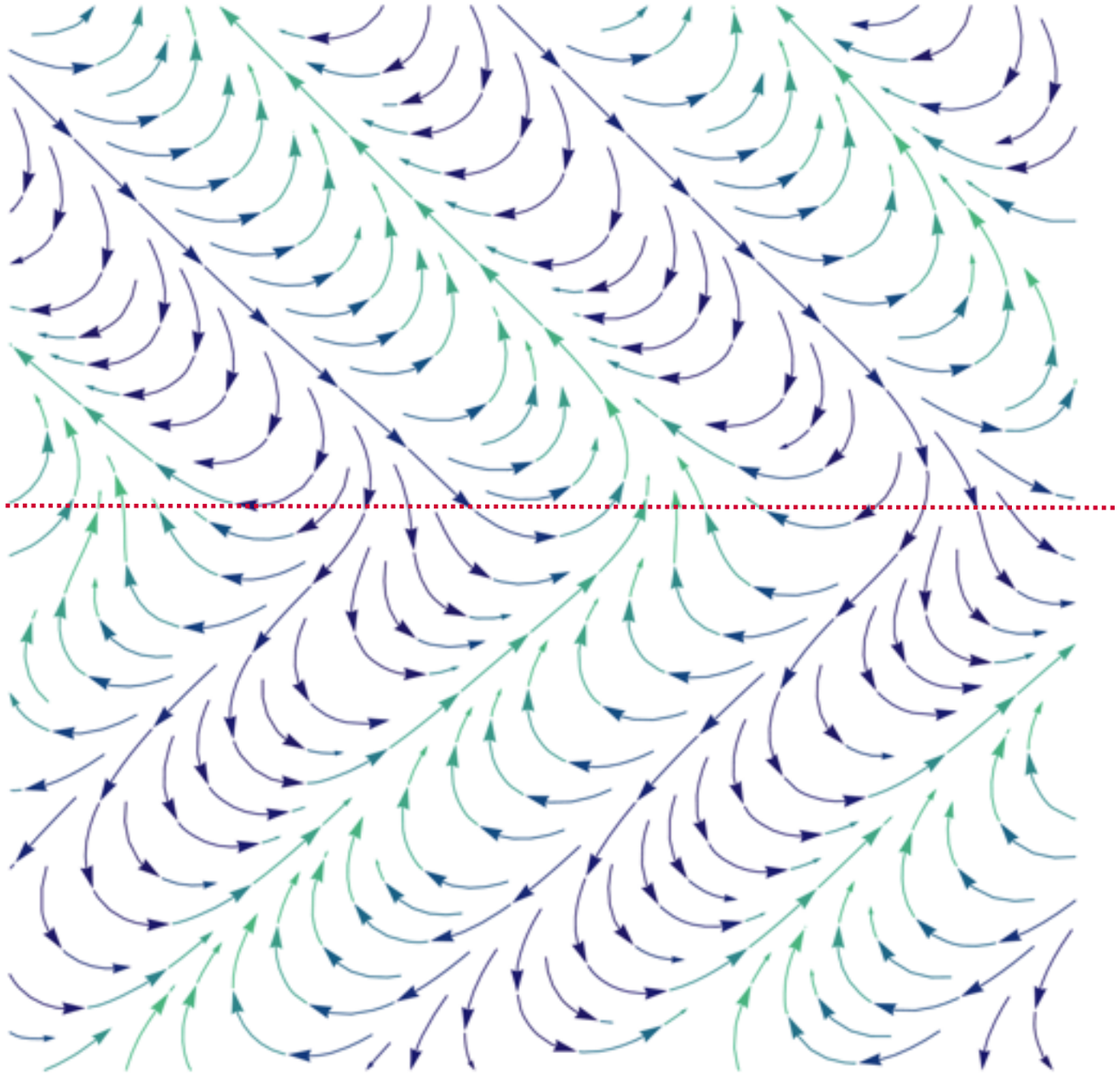

Domain wall is not bisector to the wave vectors of the adjacent domains

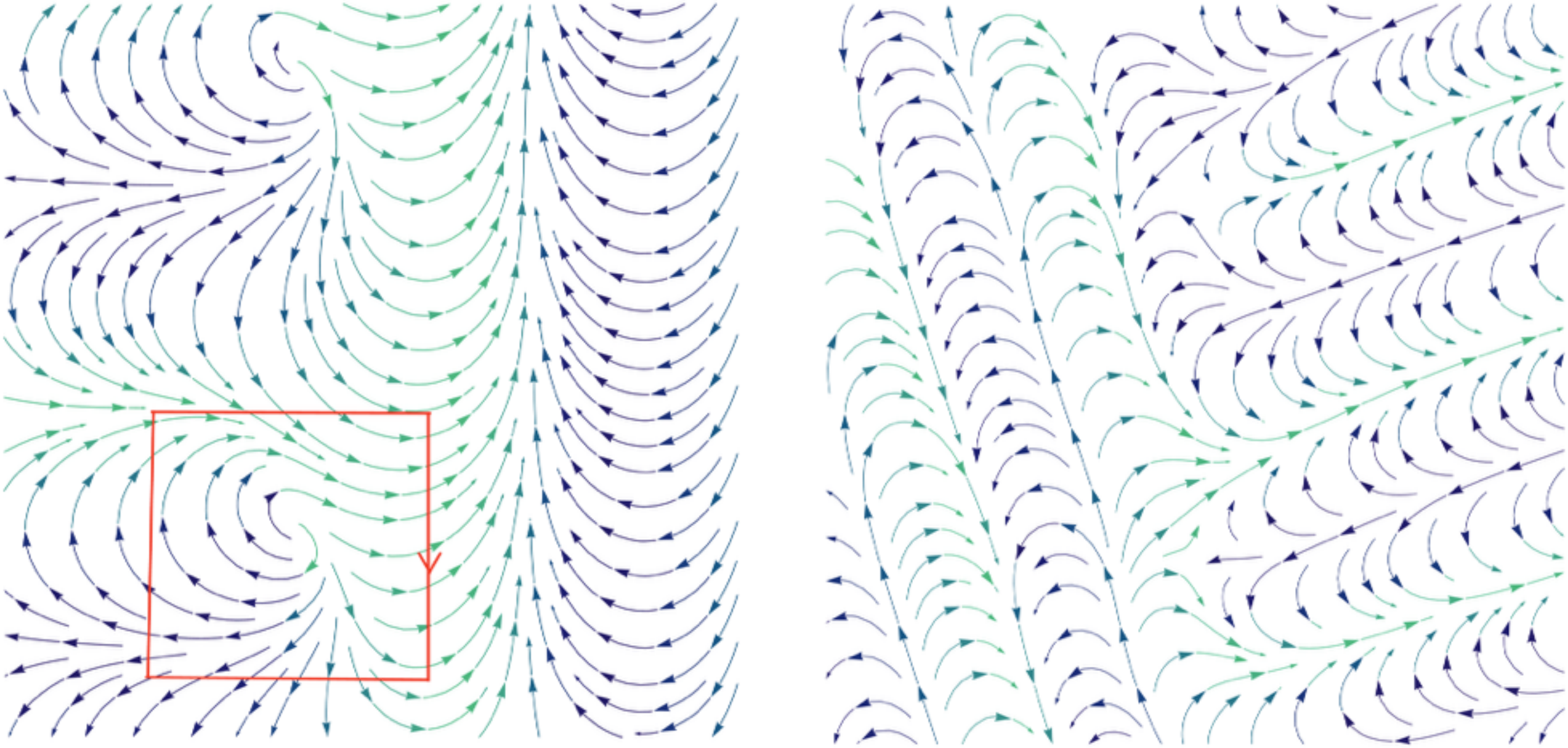

Numerically calculated vortex domain wall

Vortex domain walls much heavier than Hubert walls,
may decay in zig-zag structure of vortex-free domain walls

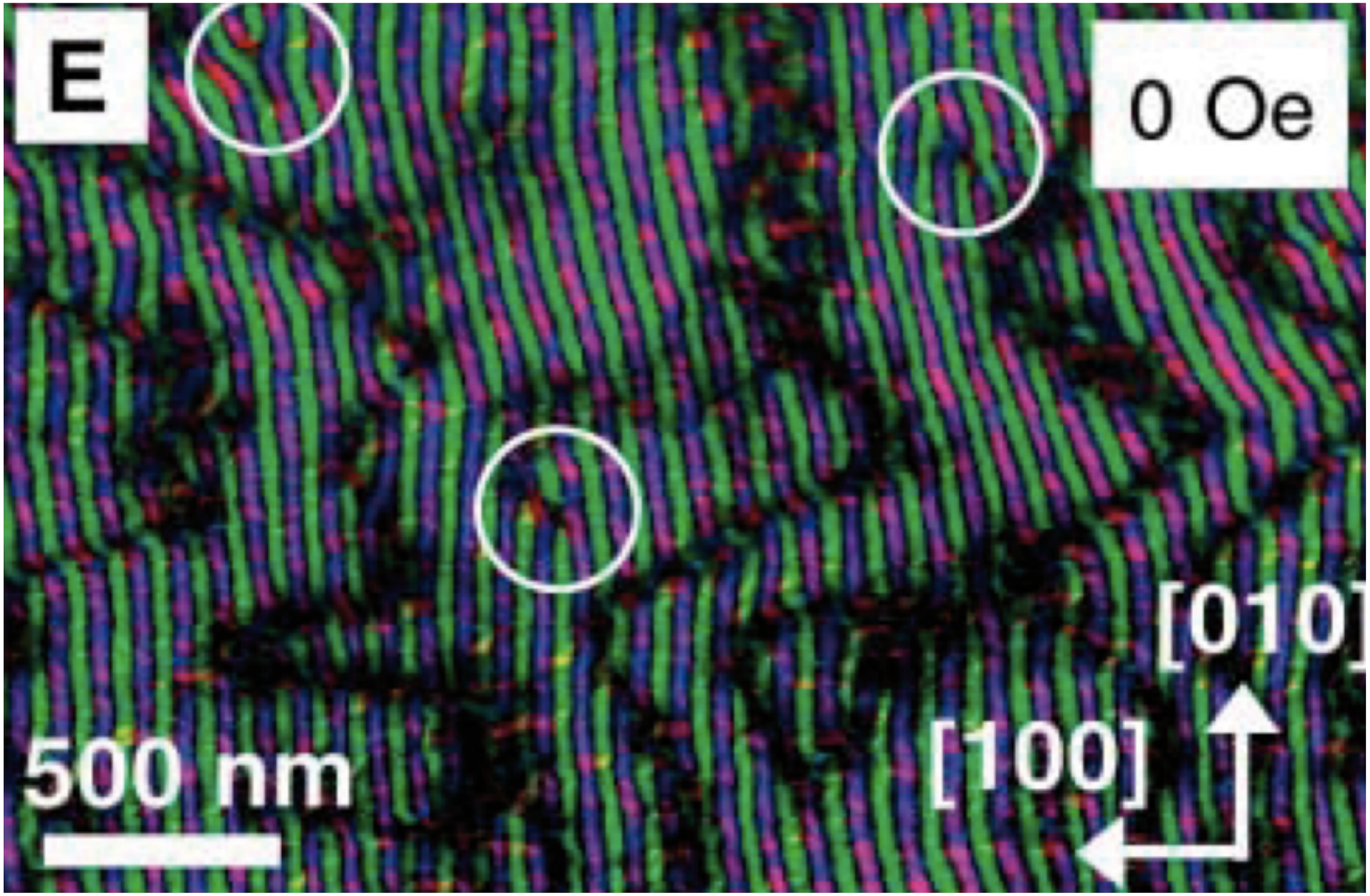

Real-Space Observation of Helical Spin Order

Masaya Uchida,[1*] Yoshinori Onose,[1†] Yoshio Matsui,[2] Yoshinori Tokura[1,3,4]

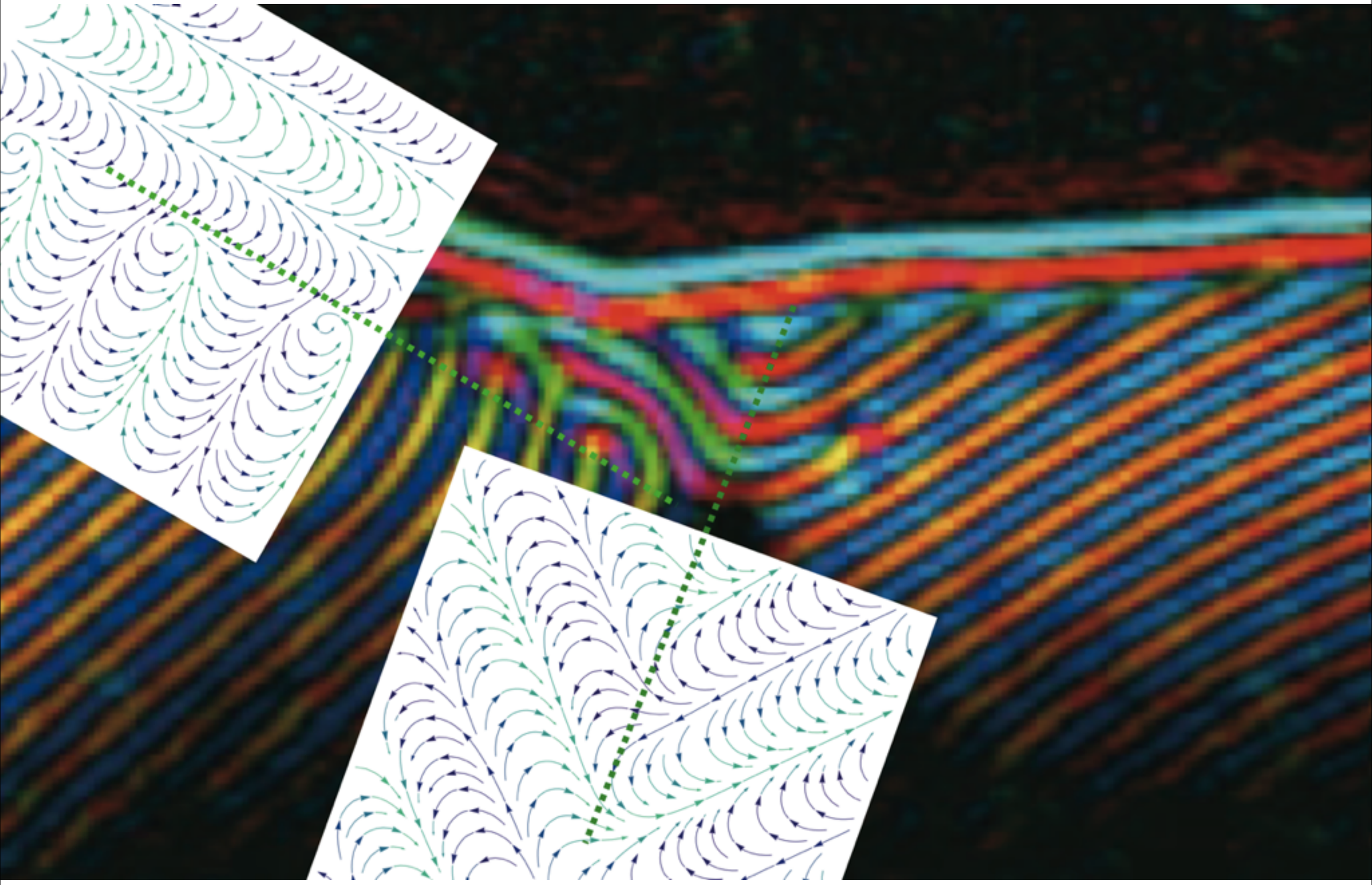

FeGe, Uchida et al. 2008

Weak pinning : Basics

Pinning by randomly distributed impurities

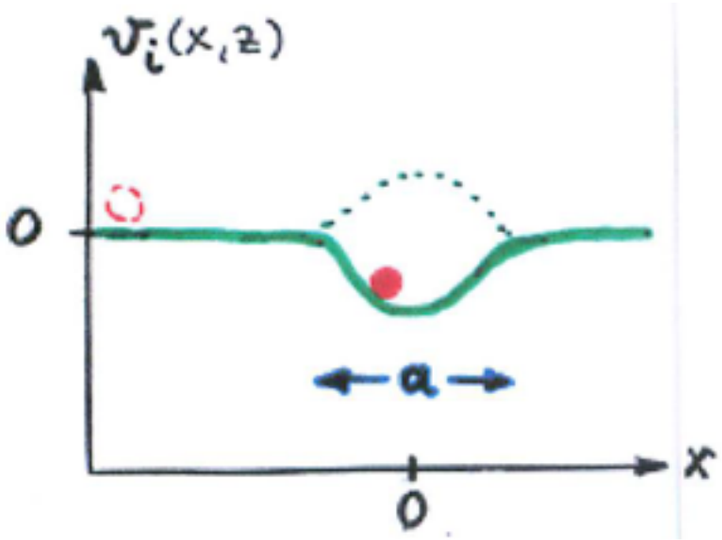

$$\mathcal{H}_{imp} = \sum_{i=1}^{N_{imp}} \int d^2\zeta \, v_{imp}\left(\boldsymbol{\zeta} - \boldsymbol{\zeta}_i, u(\boldsymbol{\zeta}) - x_i\right)$$

Pinning force due to impurity i: $f_i = -\frac{\delta \mathcal{H}_{imp}}{\delta x_i}$

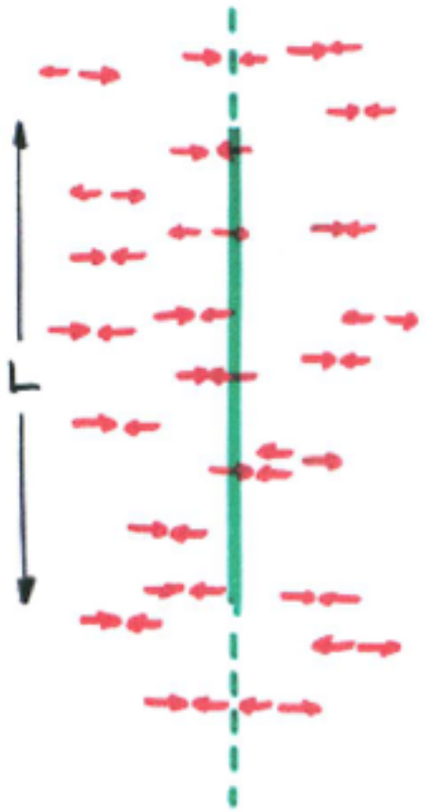

Total pinning force on rigid wall

$$\sum_{i=1}^{N_{imp}} f_i \approx \pm |f| \left(L^2 a n_{imp}\right)^{1/2} \sim L$$

Total driving force on rigid wall ~ L^2

=> no pinning of rigid walls !

Weak pinning : Basics

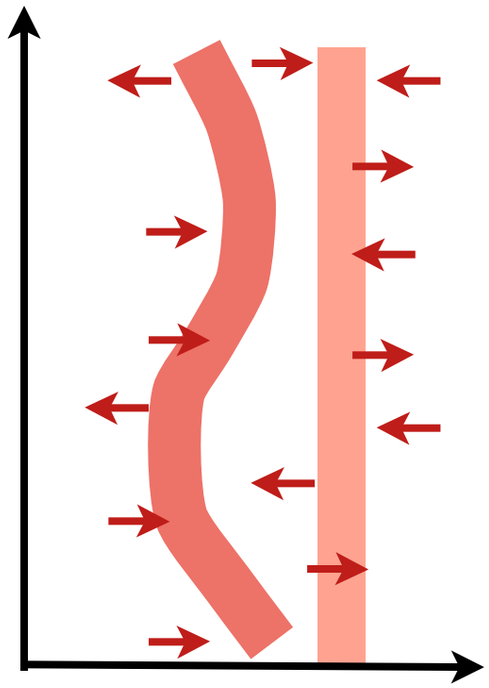

→ domain wall has to adopt elastically to pinning forces

Energy of elastic distortion u

$$E_{elast} \sim L^{\alpha} u^2$$

short range elasticity $\alpha = 0$

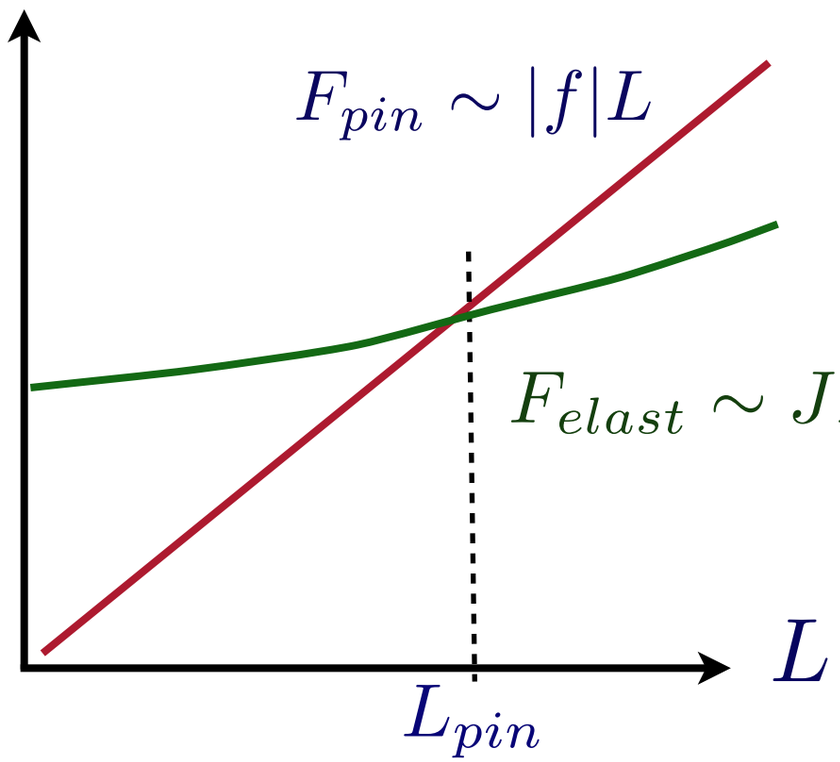

On scales L> $L_{pin} \sim (J/|f_{pin}|)^{1/(1-\alpha)}$ the domain wall decays into individually pinned regions

$$F_{pin} \sim J L_{pin}^{\alpha} \left(\frac{L}{L_{pin}} \right)^2$$

Elasticity of Hubert wall

$$\mathcal{H} = \frac{J}{2}\int d^3r \left\{ \varphi_\perp^2 + \theta^2[\varphi_x - A(\mathbf{r})]^2 + \frac{1}{4}\varphi_{xx}^2 \right\}$$

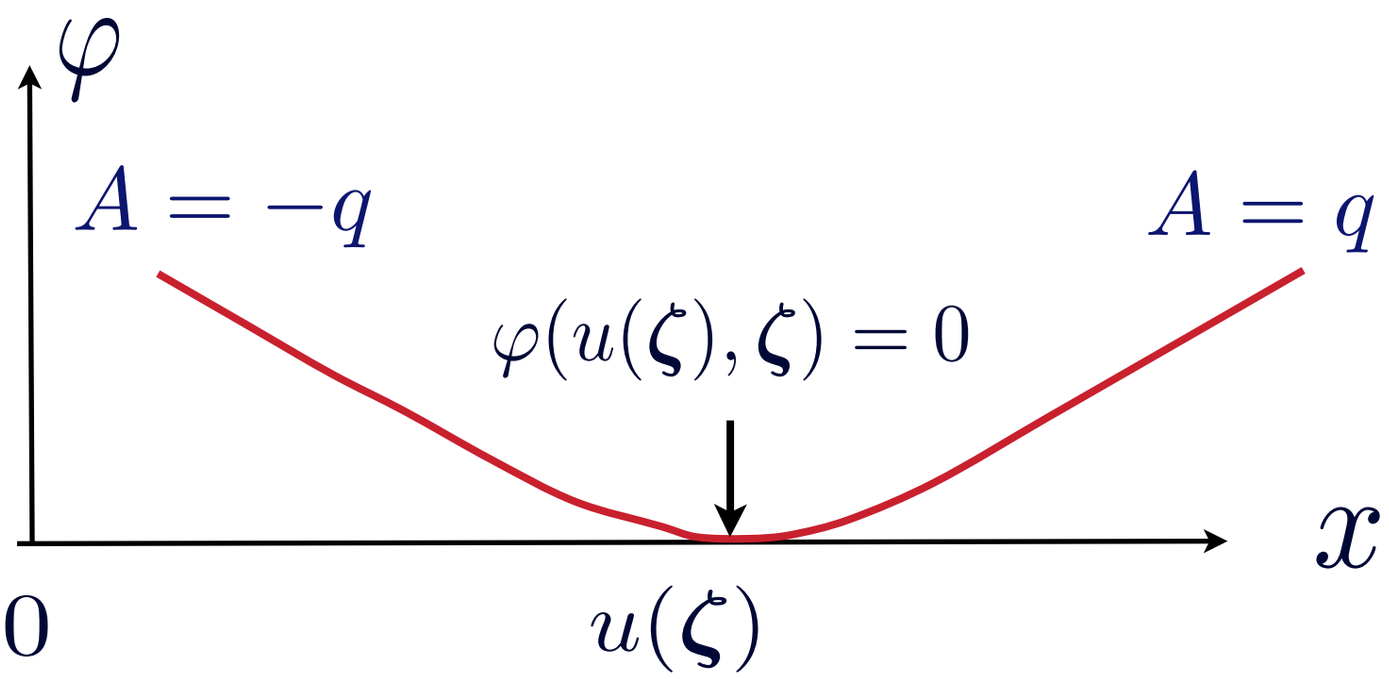

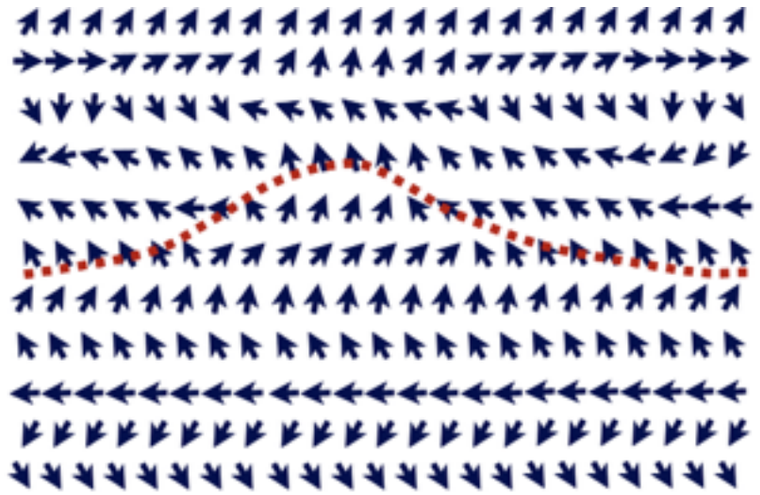

buckling (no vortices)

$$\boldsymbol{\zeta} = (y, z)$$

solution of saddle point equation

$$\varphi(\mathbf{r}) = \int_0^x dx' A(x') - q\int_{\mathbf{k}} e^{i\mathbf{k}\boldsymbol{\zeta} - |\mathbf{k}||x|/\theta} u_{\mathbf{k}}$$

long range elasticity

$$E_{elast} \sim J|\theta|^3 \sum_{\mathbf{k}} |\mathbf{k}||u_{\mathbf{k}}|^2 \sim L$$

Weak pinning - the real thing: Functional renormalization group

$$\langle f(\zeta,u)f(\zeta',u')\rangle = \delta(\zeta-\zeta')\Delta_0(u-u')$$

$$f_{\rm pin} = -\Delta_0'(u\to\pm 0)\mathcal{G}(0)$$

$$\frac{d\Delta_\ell(u)}{d\ell} = c\frac{d^2}{du^2}\Delta_\ell(u)\left[2\Delta_\ell(0)-\Delta_\ell(u)\right]$$

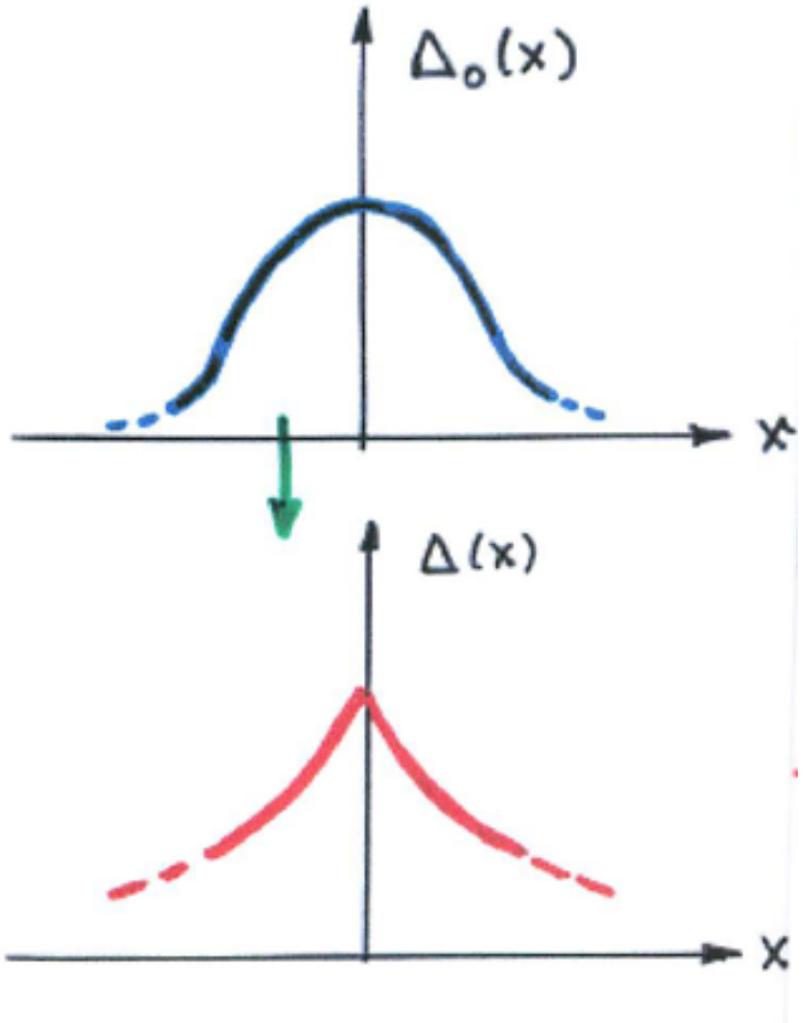

develops cusp at $\mathcal{L} = a\exp[1/(6cg_0)]$

$$|f_{\rm pin}^{(H)}| \approx \frac{64\pi J|\theta|^3}{a^3}\exp[-c_1/(|\theta|^5 c_{\rm imp})]$$

Bulk pinning of Hubert walls

weak in plane anisotropy

$$v\cos(p\varphi) \quad \rightarrow \quad \theta(x) \approx \theta\left[1 - (v/\theta^4)\sin p(qx + \varphi_0)\right]$$

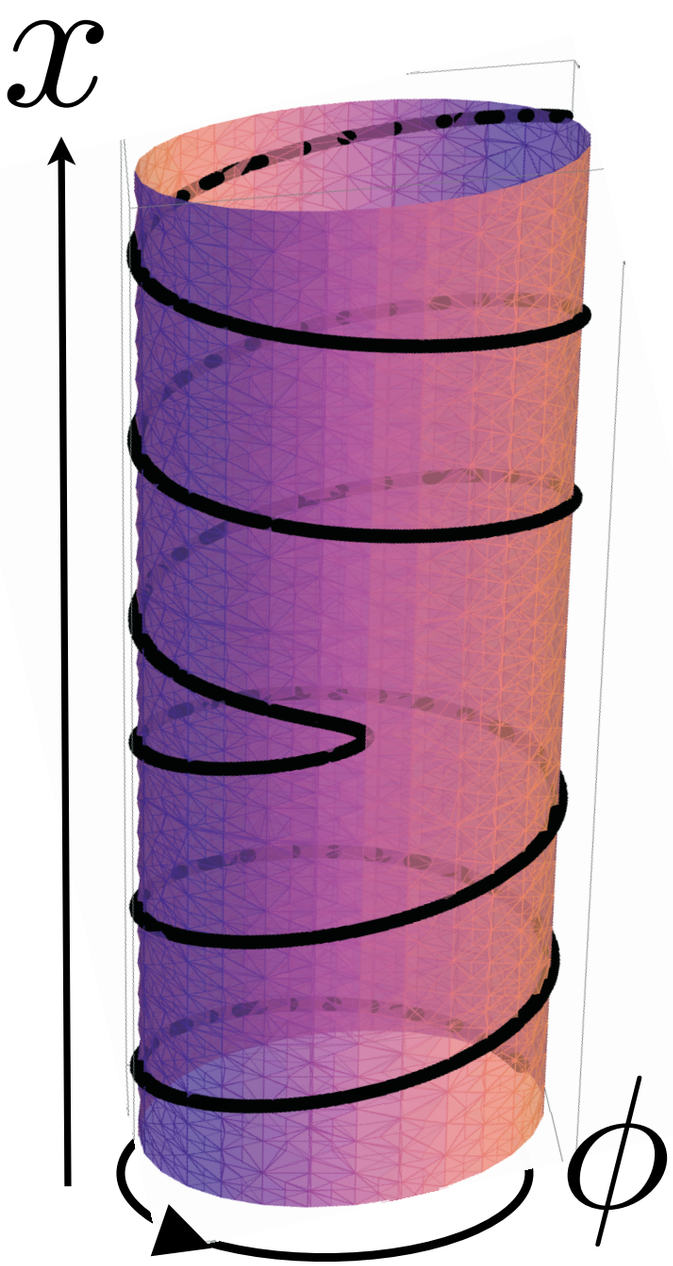

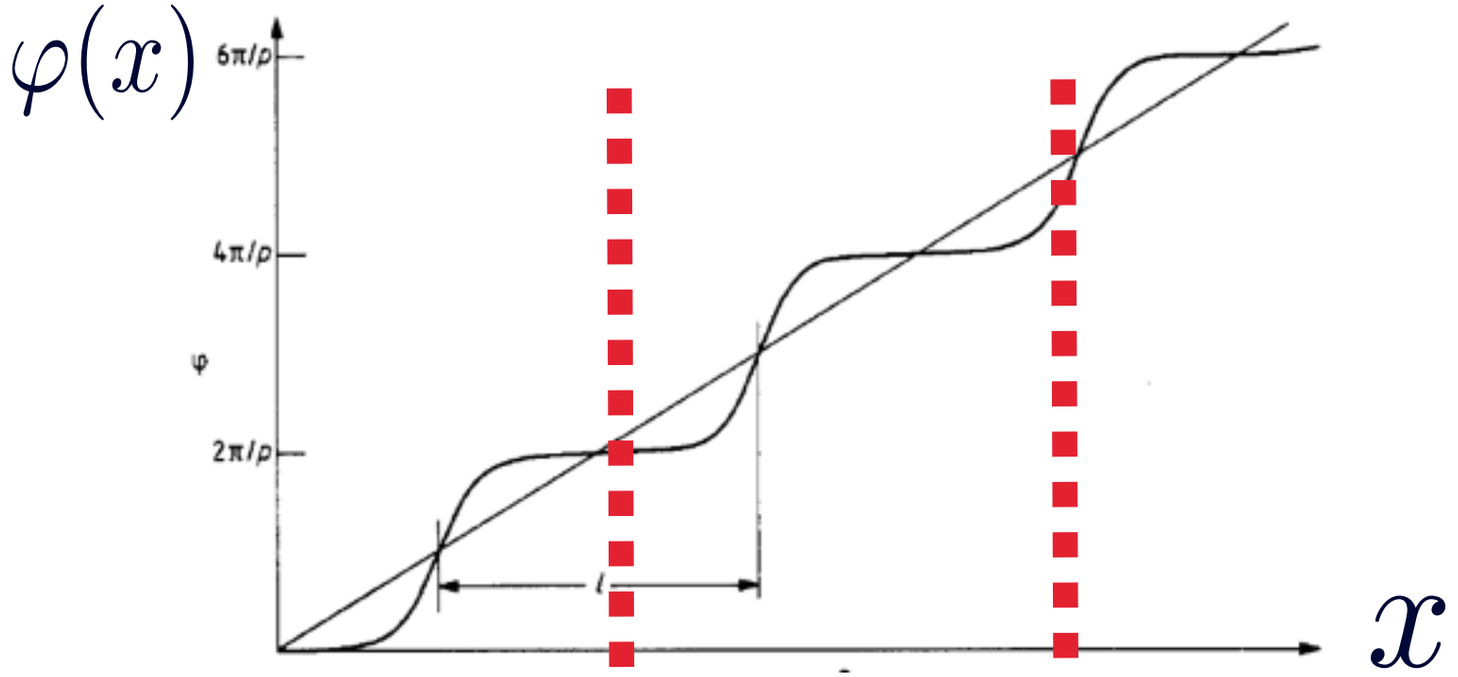

$$f_{\rm pin}^{(H,{\rm bulk})} \approx J v^4 c_{\rm imp}^2 L_x/(\pi^2 a^4 |\theta|^5).$$

Conclusions

Chiral molecules and solids are the result of spontaneous symmetry breaking and/or decoherence effects.

Chiral magnets exhibit broken time and space inversion symmetry. These symmetry breakings can appear sequentially or simultaneously.

Topological defects in chiral magnets are vortices, domain walls and skyrmion lattices.

Domain walls in helical magnets are always two dimensional textures (vortex lines), in contrast to Bloch or Neel walls, with the exception of special orientations (Hubert walls).